Rigid Body Localization Using Sensor Networks

Sundeep Prabhakar Chepuri, *Student Member, IEEE*, Geert Leus, *Fellow, IEEE*, and Alle-Jan van der Veen, *Fellow, IEEE*

***Abstract*—A framework for joint position and orientation estimation of a rigid body using range measurements is proposed. We consider a setup in which a few sensors are mounted on a rigid body. The absolute position of the rigid body is not known. However, we know how the sensors are mounted on the rigid body, i.e., the sensor topology is known. The rigid body is localized using noisy range measurements between the sensors and a few anchors (nodes with known absolute positions), and without using any inertial measurements. We propose a least-squares (LS), and a number of constrained LS estimators, where the constrained estimators solve an optimization problem on the Stiefel manifold. As a benchmark, we derive a unitarily constrained Cramér–Rao bound. Finally, the known topology of the sensors can be perturbed during fabrication or if the body is not entirely rigid. To take these perturbations into account, constrained total-least-squares estimators are also proposed.**

***Index Terms*—Constrained Cramér–Rao bound, constrained least-squares, constrained total-least-squares, rigid body localization, sensor networks, Stiefel manifold, unitary constraints.**

I. Introduction

OVER the past decade, advances in wireless sensor technology have enabled the usage of wireless sensor networks (WSNs) in different areas related to sensing, monitoring, and control. Wireless sensors are nodes equipped with a radio transceiver and a processor, capable of wireless communications and computational operations. A majority of the applications that use WSNs rely on a fundamental aspect of either associating the location information to the data that is acquired by spatially distributed sensors (e.g., in environment monitoring), or to identify the location of the sensor itself (e.g., in security, rescue, logistics). Identifying the sensor's location is a well-studied topic [2]–[4], and it is commonly referred to as sensor localization.

Localization can be either absolute or relative. In absolute localization, the aim is to estimate the absolute position of the sensor(s) using a few reference nodes whose absolute positions are known. Hence, these reference nodes are commonly referred to as *anchors*. Absolute localization problems are typically solved using measurements from certain physical phenomena, e.g., time-of-arrival (TOA), time-difference-of-arrival (TDOA), received signal strength (RSS), or angle-of-arrival (AOA) [2]–[6]. Localization can also be relative, in which case the aim is to estimate the constellation of the sensors or the topology of the network, and determining the location of a sensor relative to the other sensors is sufficient. Classical solutions to relative localization are based on multi-dimensional scaling (MDS) using squared-range measurements [7], [8]. There exists a plethora of algorithms based on these two localization paradigms, and they recently gained a lot of interest to facilitate low-power and efficient localization solutions especially in global positioning system (GPS) denied environments.

In this paper, we take a step forward from the classical sensor localization, and provide a different flavor of localization, called *rigid body localization*. In rigid body localization, we use a few sensors on a rigid body and exploit the knowledge of how the sensors are mounted on the body to jointly estimate the position as well as the orientation of the rigid body.

A. Applications and Prior Works

Rigid body localization has potential applications in a variety of fields. To list a few, it is useful for location services involving underwater (or in-liquid) systems, orbiting satellites, mechatronic systems, aircrafts, underwater vehicles, ships, robotic systems, or automobiles. In such applications, classical localization of the node(s) is not sufficient. For example, in an autonomous underwater vehicle (AUV), or an orbiting satellite, the sensing platform is not only subject to motion but also to rotation. Hence, next to position, determining the orientation of the body also forms a key component, and is essential for controlling, maneuvering, and monitoring purposes.

The orientation is sometimes referred to as attitude (aerospace applications) or tilt (for industrial equipments and consumer devices). Traditionally, position and orientation are treated separately even though they are closely related. The orientation of a body is usually measured using inertial measurement units (IMUs) comprised of accelerometers [9] and gyroscopes. However, IMUs generally suffer from accumulated errors often referred to as drift errors. The drift calibration is typically achieved using different sensor technologies including vision, magnetometers, ultra wide band (UWB), or GPS [10], [11], leading to dependencies between these technologies. Sometimes these different sensors cannot be coherently fused, for instance magnetometer based calibration needs an undistorted magnetic environment, which is typically difficult to guarantee.

Manuscript received September 30, 2013; revised April 11, 2014; accepted June 20, 2014. Date of publication July 08, 2014; date of current version August 21, 2014. The associate editor coordinating the review of this manuscript and approving it for publication was Prof. Akbar Sayeed. This work was supported in part by STW under the FASTCOM project (10551) and in part by NWO-STW under the VICI program(10382). This paper was presented in part at the International Conference on Acoustics, Speech, and Signal Processing (ICASSP), Vancouver, Canada, May 2013 [1].

The authors are with the Faculty of Electrical Engineering, Mathematics and Computer Science, Delft University of Technology, The Netherlands (e-mail: s.p.chepuri,g@tudelft.nl; j.t.leus@tudelft.nl; a.j.vanderveen@tudelft.nl).

Digital Object Identifier 10.1109/TSP.2014.2336621

GPS-based attitude determination [12]–[14] is closely related to our work, in which multiple antennas on a platform are used. Here, the attitude is estimated from GPS carrier phase measurements which involves a complicated integer problem with no unique solution in general.

B. Contributions

We propose a framework for joint position and orientation estimation of a rigid body in a three-dimensional space by borrowing techniques from classical sensor localization, i.e., using only *range* measurements between all the sensor-anchor pairs. We consider a rigid body on which a few sensor nodes are mounted. The absolute position of the rigid body is not known. However, the topology of how the sensors are mounted on the rigid body is known up to a certain accuracy. The orientation of the rigid body is expressed as a *rotation matrix* and the absolute position of the rigid body (instead of the absolute position of each individual sensor) as a *translation* vector. In other words, the absolute position of the sensors is expressed as an affine function of the Stiefel manifold.

The maximum likelihood (ML) estimators for the original problem involve solving a constrained (non-convex) non-linear least-squares (NLS) problem, which is in general difficult to solve. In order to simplify this problem, we linearize the problem by squaring the measurements. We use the linearized model in a least-squares (LS) estimator to jointly estimate the rotation matrix (to begin with, its structure is ignored) and the translation vector. Since rotation matrices are unitary matrices, we also propose a unitarily constrained least-squares (CLS) estimator and a simplified unitarily constrained least-squares (SCLS) estimator, both of which solve an optimization problem on the Stiefel manifold. The solutions from the proposed estimators can be used as an initialization to solve the maximum-likelihood estimators or the original non-linear LS problem if needed. We also derive a unitarily constrained Cramér–Rao bound (CCRB), which is used as a benchmark for the proposed estimators.

In many applications, the sensor topology might not be accurately known, i.e., the known topology can be noisy. These perturbations are typically introduced while mounting the sensors during fabrication or if the body is not entirely rigid. To account for such perturbations, we propose a unitarily constrained total-least-squares (CTLS) estimator and a simplified unitarily constrained total-least-squares (SCTLS) estimator. The performance of the proposed estimators is analyzed using simulations. Using a sensor array with a known geometry not only enables orientation estimation, but also yields a better localization performance. The initial results on rigid body localization using range measurements, viz., SCLS and SCTLS were proposed in [1].

The proposed framework of rigid body localization can also be used as an add-on to the existing IMU based systems to correct the drift errors, or in environments where inertial measurements and/or positioning via GPS is not feasible. The proposed framework is based on a static position and orientation, unlike most of the orientation estimators which are based on inertial measurements and a certain dynamical state-space model (e.g., see [10]). Hence, our approach is useful when there is no dynamic model available. We should stress, however, that the proposed framework is also suitable for the estimation (tracking) of dynamic position and orientation using a state-constrained Kalman filter for instance, and some initial results on this topic can be found in [15].

C. Outline and Notations

The remainder of the paper is organized as follows. The considered problem is described in Section II. The LS estimators based on perfect knowledge of the sensor topology are discussed in Section III, and the unitarily constrained Cramér–Rao bound is derived in Section IV. The TLS estimators to account for perturbations on the topology are discussed in Section V. Numerical results based on simulations are provided in Section VI. Finally, the paper concludes with some remarks in Section VII.

The notations used in this paper are described as follows. Upper (lower) bold face letters are used for matrices (column vectors). $(\cdot)^T$ denotes transposition. $\mathrm{diag}(\cdot)$ refers to a block diagonal matrix with the elements in its argument on the main diagonal. $\mathbf{1}_N$ $(\mathbf{0}_N)$ denotes the $N \times 1$ vector of ones (zeros). $\mathbf{I}_N$ is an identity matrix of size N. $\mathbb{E}\{\cdot\}$ denotes the expectation operation. $\otimes$ is the Kronecker product. $(\cdot)^\dagger$ denotes the pseudo inverse, i.e., for a full column-rank tall matrix $\mathbf{A}$ the pseudo inverse (or the left-inverse) is given by $\mathbf{A}^\dagger = (\mathbf{A}^T\mathbf{A})^{-1}\mathbf{A}^T$, and for a full row-rank wide matrix $\mathbf{A}$ the pseudo inverse (or the right-inverse) is given by $\mathbf{A}^\dagger = \mathbf{A}^T(\mathbf{A}\mathbf{A}^T)^{-1}$. The right- or left-inverse will be clear from the context. $\mathrm{vec}(\cdot)$ is an $MN \times 1$ vector formed by stacking the columns of its matrix argument of size $M \times N$. $\mathrm{unvec}(\cdot)$ is an $M \times N$ matrix formed by the inverse $\mathrm{vec}(\cdot)$ operation on an $MN \times 1$ vector. $\mathrm{cond}(\mathbf{A})$ denotes the condition number of a matrix $\mathbf{A}$. We use the matrix property $\mathrm{vec}(\mathbf{ABC}) = (\mathbf{C}^T \otimes \mathbf{A})\mathrm{vec}(\mathbf{B})$. Further, $\mathbf{a}^{\odot 2}$ denotes the element-wise squaring of a vector $\mathbf{a}$, and $\mathrm{tr}\{\cdot\}$ denotes the matrix trace operator. A covariance matrix is denoted by bold upper case $\mathbf{R}$ with specified subscripts: $\mathbf{R}_\mathbf{n}$ denotes the covariance matrix of a random vector $\mathbf{n}$. Finally, $\mathbf{R}_\mathbf{n}^{1/2}$ is defined from the Cholesky decomposition $\mathbf{R}_\mathbf{n} := \mathbf{R}_\mathbf{n}^{1/2}\mathbf{R}_\mathbf{n}^{T/2}$.

II. Problem Formulation and Modeling

A. Problem Formulation

Consider a network with M anchors (nodes with known absolute locations) and N sensors in a 3-dimensional space. The sensors are mounted on a rigid body as illustrated in Fig. 1. The wireless sensors are mounted on the rigid body (e.g., at the factory), and the topology of how these sensors are mounted is known up to a certain accuracy. In other words, we connect a so-called *reference frame* to the rigid body, as illustrated in Fig. 1, and in that reference frame, the coordinates of the nth sensor are given by the known 3×1 vector $\mathbf{c}_n = [c_{n,1}, c_{n,2}, c_{n,3}]^T$. The sensor topology is basically determined by the matrix $\mathbf{C} = [\mathbf{c}_1, \mathbf{c}_2, \ldots, \mathbf{c}_N] \in \mathbb{R}^{3 \times N}$. Let the absolute coordinates of the mth anchor and the nth sensor be denoted by a 3×1 vector $\mathbf{a}_m$ and $\mathbf{s}_n$, respectively, where $\mathbf{s}_n$ is not known. The absolute positions of the anchors and the sensors

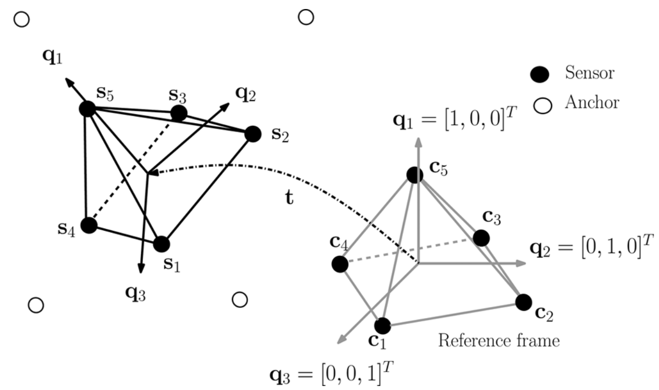

Fig. 1. An illustration of the sensors on a rigid body undergoing a rotation and translation.

are collected in the matrices $\mathbf{A} = [\mathbf{a}_1, \mathbf{a}_2, \ldots, \mathbf{a}_M] \in \mathbb{R}^{3\times M}$ and $\mathbf{S} = [\mathbf{s}_1, \mathbf{s}_2, \ldots, \mathbf{s}_N] \in \mathbb{R}^{3\times N}$, respectively.

1) Rigid Body Transformation: A Stiefel manifold [16] in three dimensions, denoted by $\mathcal{V}_{3,3}$, is the set of all 3×3 unitary matrices $\mathbf{Q} = [\mathbf{q}_1, \mathbf{q}_2, \mathbf{q}_3] \in \mathbb{R}^{3\times 3}$, i.e.,

$$\mathcal{V}_{3,3} = \{\mathbf{Q} \in \mathbb{R}^{3\times 3} : \mathbf{Q}^T\mathbf{Q} = \mathbf{Q}\mathbf{Q}^T = \mathbf{I}_3\}.$$

The absolute position of the nth sensor can be written as an affine function of a point on the Stiefel manifold, i.e.,

$$\begin{aligned} \mathbf{s}_n &= c_{n,1}\mathbf{q}_1 + c_{n,2}\mathbf{q}_2 + c_{n,3}\mathbf{q}_3 + \mathbf{t} \\ &= \mathbf{Q}\mathbf{c}_n + \mathbf{t}, \end{aligned} \tag{1}$$

where $\mathbf{t} \in \mathbb{R}^{3\times 1}$ denotes the unknown translation. More specifically, the parameter vector $\mathbf{t}$ refers to the unknown position of the rigid body. The combining weights $\mathbf{c}_n$ are the *known* coordinates of the nth sensor in the reference frame. This means that the unknown unitary matrix $\mathbf{Q}$ actually tells us how the rigid body has rotated in the reference frame. When there is no rotation, then we have $\mathbf{Q} = \mathbf{I}_3$. The relation in (1) is sometimes also referred to as the *rigid body transformation*. The rotation matrices can uniquely represent the orientation of a rigid body unlike Euler angles or unit quaternions (see [17] for more details). The rigid body transformation is also used in computer vision applications [18]–[20].

With (1), the absolute position of all the sensors can be written as

$$\mathbf{S} = \mathbf{Q}\mathbf{C} + \mathbf{t}\mathbf{1}_N^T = \overbrace{[\mathbf{Q} \mid \mathbf{t}]}^{\boldsymbol{\Theta}} \overbrace{\left[\frac{\mathbf{C}}{\mathbf{1}_N^T}\right]}^{\mathbf{C}_e}, \tag{2}$$

where $\boldsymbol{\Theta} \in \mathbb{R}^{3\times 4}$ is the unknown transformation matrix.

2) Range Measurements: The proposed framework is general and can be applied to range estimates obtained from any one of the standard ranging techniques (e.g., two-way ranging based on TOA measurements [2], [5]). The framework is valid as long as the range estimates between all the sensor-anchor pairs are available. Further, we assume that the body position is nearly static during the ranging process, i.e., the linear and angular velocities are negligible compared to the propagation speed.

Let the range (or the Euclidean distance) between the mth anchor and the nth sensor be denoted by $\rho_{mn} = \|\mathbf{a}_m - \mathbf{s}_n\|_2$. The noisy range measurement between the mth anchor and the nth sensor can be expressed as

$$\begin{aligned} y_{mn} &= \|\mathbf{a}_m - \mathbf{s}_n\|_2 + v_{mn} \\ &= \|\mathbf{a}_m - (\mathbf{Q}\mathbf{c}_n + \mathbf{t})\|_2 + v_{mn}, \end{aligned} \tag{3}$$

where $v_{mn} \sim \mathcal{N}(0, \sigma_{mn}^2)$ is the stochastic noise resulting from the ranging process. The ranging noise $v_{mn}, m = 1, 2, \ldots, M$; $n = 1, 2, \ldots, N$, is a sequence of independent random variables whose variance σ_{mn}^2 is assumed to be known or easily estimated.

3) Problem Statement: Having introduced the rigid body transformation in (1) and the measurement model (3) we can now formally state the rigid body localization problem as follows.

Problem statement (Rigid Body Localization): Given one range measurement between each sensor-anchor pair, i.e., y_{mn} as in (3), the ranging noise variance σ_{mn}^2, for $m = 1, 2, \ldots, M$ and $n = 1, 2, \ldots, N$, the positions of the anchors $\mathbf{A}$, and the topology of the sensors on the rigid body determined by the matrix $\mathbf{C}$, jointly estimate the position $\mathbf{t} \in \mathbb{R}^{3\times 1}$ and orientation $\mathbf{Q} \in \mathcal{V}_{3,3}$ of the rigid body.

The ML estimator for jointly estimating the orientation and translation is to solve the following optimization problem

$$\arg\min_{\mathbf{Q},\mathbf{t}} \sum_{m=1}^{M}\sum_{n=1}^{N} \sigma_{mn}^{-2}(y_{mn} - \|\mathbf{a}_m - (\mathbf{Q}\mathbf{c}_n + \mathbf{t})\|_2)^2 \tag{4a}$$

$$\text{s.t.} \quad \mathbf{Q}^T\mathbf{Q} = \mathbf{I}_3. \tag{4b}$$

The above problem is a non-linear and a non-convex optimization problem, and is in general difficult to solve. To simplify this problem, we next linearize the model in (3), which can then be solved using linear LS based estimators. The solution from the proposed estimators can then be used as an initialization to solve the above NLS problem if needed.

B. Squared-Range Measurements

The model in (3) is non-linear in $\mathbf{s}_n$, $\mathbf{Q}$, and $\mathbf{t}$. Therefore, we linearize the non-linear model in (3) by squaring it. Squaring the measurements in (3) results in a noise term with a non-negative known mean[1] σ_{mn}^2. Subtracting that mean σ_{mn}^2 from the squared-range measurements between the mth anchor and the nth sensor, we obtain

$$\begin{aligned} d_{mn} &= y_{mn}^2 - \sigma_{mn}^2 \\ &= \|\mathbf{a}_m\|_2^2 - 2\mathbf{a}_m^T\mathbf{s}_n + \|\mathbf{s}_n\|_2^2 + n_{mn}, \end{aligned} \tag{5}$$

where

$$n_{mn} = 2\rho_{mn}v_{mn} + v_{mn}^2 - \sigma_{mn}^2 \tag{6}$$

[1]For low noise levels, this non-negative mean which is simply the variance of the range error in (3) can be ignored.

is the new zero-mean noise term due to squaring. Collecting these new squared-range measurements between the nth sensor and all the anchors in

$$\mathbf{d}_n = [d_{1n}, d_{2n}, \ldots, d_{Mn}]^T \in \mathbb{R}^{M\times 1},$$

we can write (5) in a vector form as

$$\mathbf{d}_n = \boldsymbol{\alpha} - 2\mathbf{A}^T\mathbf{s}_n + \|\mathbf{s}_n\|_2^2\mathbf{1}_M + \mathbf{n}_n, \tag{7}$$

where

$$\boldsymbol{\alpha} = [\|\mathbf{a}_1\|_2^2, \|\mathbf{a}_2\|_2^2, \ldots, \|\mathbf{a}_M\|_2^2]^T \in \mathbb{R}^{M\times 1},$$

is known, and

$$\mathbf{n}_n = [n_{1n}, n_{2n}, \ldots, n_{Mn}]^T \in \mathbb{R}^{M\times 1}.$$

Subtracting the knowns in (7) from the measurements, we arrive at

$$\mathbf{d}_n - \boldsymbol{\alpha} = -2\mathbf{A}^T\mathbf{s}_n + \|\mathbf{s}_n\|_2^2\mathbf{1}_M + \mathbf{n}_n. \tag{8}$$

We next eliminate the vector $\|\mathbf{s}_n\|_2^2\mathbf{1}_M$ in (8) using an isometry decomposition of the projection matrix

$$\mathbf{P}_M = \mathbf{I}_M - \frac{1}{M}\mathbf{1}_M\mathbf{1}_M^T = \mathbf{U}_M\mathbf{U}_M^T \in \mathbb{R}^{M\times M},$$

where $\mathbf{U}_M$ is an $M \times (M-1)$ matrix obtained by collecting orthonormal basis vectors of the null-space of $\mathbf{1}_M$ such that $\mathbf{U}_M^T\mathbf{1}_M = \mathbf{0}_{M-1}$. Pre-multiplying both sides of (8) with $\mathbf{U}_M^T$, we arrive at

$$\mathbf{U}_M^T(\mathbf{d}_n - \boldsymbol{\alpha}) = -2\mathbf{U}_M^T\mathbf{A}^T\mathbf{s}_n + \mathbf{U}_M^T\mathbf{n}_n. \tag{9}$$

Stacking (9) for all the N sensors, we obtain

$$\mathbf{U}_M^T\mathbf{D} = -2\mathbf{U}_M^T\mathbf{A}^T\mathbf{S} + \mathbf{U}_M^T\mathbf{N}, \tag{10}$$

where we define the following $M \times N$ matrices:

$$\begin{aligned} \mathbf{D} &= [\mathbf{d}_1, \mathbf{d}_2, \ldots, \mathbf{d}_N] - \boldsymbol{\alpha}\mathbf{1}_N^T, \\ \text{and} \quad \mathbf{N} &= [\mathbf{n}_1, \mathbf{n}_2, \ldots, \mathbf{n}_N]. \end{aligned}$$

The linear model in (10) can then be compactly expressed as

$$\bar{\mathbf{D}} = \bar{\mathbf{A}}\mathbf{S} + \bar{\mathbf{N}}, \tag{11}$$

where we have introduced the following matrices:

$$\begin{aligned} \bar{\mathbf{D}} &= \mathbf{U}_M^T\mathbf{D} \in \mathbb{R}^{(M-1)\times N}, \\ \bar{\mathbf{A}} &= -2\mathbf{U}_M^T\mathbf{A}^T \in \mathbb{R}^{(M-1)\times 3}, \\ \text{and} \quad \bar{\mathbf{N}} &= \mathbf{U}_M^T\mathbf{N} \in \mathbb{R}^{(M-1)\times N}. \end{aligned}$$

Vectorizing (11) leads to

$$\bar{\mathbf{d}} = \overbrace{(\mathbf{I}_N \otimes \bar{\mathbf{A}})}^{(M-1)N\times 3N} \mathbf{s} + \bar{\mathbf{n}}, \tag{12}$$

where

$$\begin{aligned} \mathbf{s} &= \mathrm{vec}(\mathbf{S}) \in \mathbb{R}^{3N}, \\ \bar{\mathbf{d}} &= \mathrm{vec}(\bar{\mathbf{D}}) \in \mathbb{R}^{(M-1)N}, \\ \text{and} \quad \bar{\mathbf{n}} &= \mathrm{vec}(\bar{\mathbf{N}}) = (\mathbf{I}_N \otimes \mathbf{U}_M^T)\mathrm{vec}(\mathbf{N}) \in \mathbb{R}^{(M-1)N}. \end{aligned}$$

Using the rigid body transformation in (2), we can relate the measurements $\bar{\mathbf{D}}$ in (11) and the transformation matrix $\boldsymbol{\Theta}$. Substituting (2) in (11), we arrive at the following linear model

$$\bar{\mathbf{D}} = \bar{\mathbf{A}}\boldsymbol{\Theta}\mathbf{C}_{\mathrm{e}} + \bar{\mathbf{N}}, \tag{13}$$

which can then be vectorized to

$$\bar{\mathbf{d}} = \overbrace{(\mathbf{C}_{\mathrm{e}}^T \otimes \bar{\mathbf{A}})}^{(M-1)N\times 9}\boldsymbol{\theta} + \bar{\mathbf{n}}, \tag{14}$$

where

$$\boldsymbol{\theta} = \mathrm{vec}(\boldsymbol{\Theta}) = [\mathbf{q}_1^T, \mathbf{q}_2^T, \mathbf{q}_3^T, \mathbf{t}^T]^T \in \mathbb{R}^{12\times 1}$$

is the unknown parameter vector that has to be estimated.

The covariance matrix of the noise $\bar{\mathbf{n}}$ in (14) is denoted by

$$\mathbf{R}_{\bar{\mathbf{n}}} = (\mathbf{I}_N \otimes \mathbf{U}_M^T)\mathbf{R}_{\mathbf{n}}(\mathbf{I}_N \otimes \mathbf{U}_M) \in \mathbb{R}^{(M-1)N\times(M-1)N},$$

where $\mathbf{R}_{\mathbf{n}}$ is the covariance matrix of $\mathbf{n} = \mathrm{vec}(\mathbf{N})$, and is developed in Appendix A. To whiten[2] the noise, the vectorized model in (14) (equivalently the model in (12)) is transformed to

$$\begin{aligned} \bar{\mathbf{d}}' &= \mathbf{R}_{\bar{\mathbf{n}}}^{-1/2}\bar{\mathbf{d}} \\ &= \mathbf{R}_{\bar{\mathbf{n}}}^{-1/2}((\mathbf{I}_N \otimes \bar{\mathbf{A}})\mathbf{s} + \bar{\mathbf{n}}) \\ &= \mathbf{R}_{\bar{\mathbf{n}}}^{-1/2}((\mathbf{C}_{\mathrm{e}}^T \otimes \bar{\mathbf{A}})\boldsymbol{\theta} + \bar{\mathbf{n}}). \end{aligned} \tag{15}$$

In the next section, we propose several estimators of $\boldsymbol{\theta}$ from the processed squared-range measurements $\bar{\mathbf{d}}'$.

III. Linear Least-Squares Estimators

To begin with, we first look at the (topology-agnostic) classical LS-based location estimator.

A. Classical LS-Based Localization (Topology-Agnostic)

We use the classical (weighted) LS estimator of $\mathbf{s}$ from $\bar{\mathbf{d}}'$ in (15) to estimate the absolute position of the sensors as

$$\begin{aligned} \widehat{\mathbf{s}}_{\mathrm{LS}} &= \arg\min_{\mathbf{s}\in\mathbb{R}^{3N}} \left\|\bar{\mathbf{d}}' - \mathbf{R}_{\bar{\mathbf{n}}}^{-1/2}(\mathbf{I}_N \otimes \bar{\mathbf{A}})\mathbf{s}\right\|_2^2 \\ &= \left(\mathbf{R}_{\bar{\mathbf{n}}}^{-1/2}(\mathbf{I}_N \otimes \bar{\mathbf{A}})\right)^{\dagger}\bar{\mathbf{d}}', \end{aligned} \tag{16}$$

which is unique if $\mathbf{I}_N \otimes \bar{\mathbf{A}}$ has full column-rank, which requires $M \geq 4$. Finally, we have

$$\widehat{\mathbf{S}}_{\mathrm{LS}} = \mathrm{unvec}(\widehat{\mathbf{s}}_{\mathrm{LS}}) \in \mathbb{R}^{3\times N}.$$

[2]The noise covariance is parameter dependent, and hence, for whitening it we use an estimated covariance matrix $\widehat{\mathbf{R}}_{\mathbf{n}}$ as discussed in Section VI.

In this classical LS-based localization, the knowledge about the known sensor topology is not exploited, and the absolute position of each sensor is estimated separately.

B. Unconstrained LS Estimator

Note that the unknown parameter vector $\boldsymbol{\theta}$ has a structure because $\mathbf{Q} = [\mathbf{q}_1, \mathbf{q}_2, \mathbf{q}_3]$ is a unitary matrix. We propose to estimate $\boldsymbol{\theta}$ ignoring its structure from $\bar{\mathbf{d}}'$ in (15) using the following (weighted) LS estimator

$$\begin{aligned}\widehat{\boldsymbol{\theta}}_{\mathrm{LS}} &= \arg\min_{\boldsymbol{\theta}} \|\bar{\mathbf{d}}' - \mathbf{R}_{\bar{\mathbf{n}}}^{-1/2}(\mathbf{C}_{\mathrm{e}}^T \otimes \bar{\mathbf{A}})\boldsymbol{\theta}\|_2^2 \\ &= \left(\mathbf{R}_{\bar{\mathbf{n}}}^{-1/2}(\mathbf{C}_{\mathrm{e}}^T \otimes \bar{\mathbf{A}})\right)^{\dagger}\bar{\mathbf{d}}'. \qquad (17)\end{aligned}$$

The estimator in (17) will have a unique solution if the matrix $\mathbf{C}_{\mathrm{e}}^T \otimes \bar{\mathbf{A}}$ has full column-rank, i.e., $\mathbf{C}_{\mathrm{e}}^T$ and $\bar{\mathbf{A}}$ are both full-column rank, and this requires $(M-1)N \geq 12$. Finally, we have

$$\widehat{\boldsymbol{\Theta}}_{\mathrm{LS}} = \mathrm{unvec}(\widehat{\boldsymbol{\theta}}_{\mathrm{LS}}) = \left[\widehat{\mathbf{Q}}_{\mathrm{LS}}\, \widehat{\mathbf{t}}_{\mathrm{LS}}\right]. \qquad (18)$$

C. Unitarily Constrained Estimators

The LS estimate $\widehat{\mathbf{Q}}_{\mathrm{LS}}$ obtained in (18) is typically (in presence of noise) not a rotation matrix. Hence, we next propose two LS estimators with a unitary constraint on $\mathbf{Q}$. Both these estimators solve an optimization problem on the Stiefel manifold.

For this purpose, we decouple the rotations and the translations in (2) by eliminating the all-one vector $\mathbf{1}_N^T$, and hence the matrix $\mathbf{t}\mathbf{1}_N^T$. In order to eliminate $\mathbf{t}\mathbf{1}_N^T$, we use an isometry matrix $\mathbf{U}_N$, and as earlier, this matrix is obtained by the isometry decomposition of $\mathbf{P}_N$, given by

$$\mathbf{P}_N = \mathbf{I}_N - \frac{1}{N}\mathbf{1}_N\mathbf{1}_N^T = \mathbf{U}_N\mathbf{U}_N^T,$$

where $\mathbf{U}_N$ is an $N \times (N-1)$ matrix obtained by collecting orthonormal basis vectors of the null-space of $\mathbf{1}_N$ such that $\mathbf{1}_N^T\mathbf{U}_N = \mathbf{0}_{N-1}^T$. Right-multiplying both sides of (2) with $\mathbf{U}_N$ leads to

$$\mathbf{S}\mathbf{U}_N = \mathbf{Q}\mathbf{C}\mathbf{U}_N. \qquad (19)$$

Combining (11) and (19) we get the following linear model

$$\bar{\mathbf{D}}\mathbf{U}_N = \bar{\mathbf{A}}\mathbf{Q}\mathbf{C}\mathbf{U}_N + \bar{\mathbf{N}}\mathbf{U}_N,$$

which can be further simplified as

$$\tilde{\mathbf{D}} = \bar{\mathbf{A}}\mathbf{Q}\bar{\mathbf{C}} + \tilde{\mathbf{N}}, \qquad (20)$$

where we have introduced the following matrices:

$$\begin{aligned}\tilde{\mathbf{D}} &= \mathbf{U}_M^T\mathbf{D}\mathbf{U}_N \in \mathbb{R}^{(M-1)\times(N-1)},\\ \bar{\mathbf{C}} &= \mathbf{C}\mathbf{U}_N \in \mathbb{R}^{3\times(N-1)},\\ \text{and}\quad \tilde{\mathbf{N}} &= \mathbf{U}_M^T\mathbf{N}\mathbf{U}_N \in \mathbb{R}^{(M-1)\times(N-1)}.\end{aligned}$$

Vectorizing (20), we obtain

$$\tilde{\mathbf{d}} = \overbrace{(\bar{\mathbf{C}}^T \otimes \bar{\mathbf{A}})}^{K\times 9}\mathbf{q} + \tilde{\mathbf{n}}, \qquad (21)$$

where $K = (M-1)(N-1)$, $\tilde{\mathbf{d}} = \mathrm{vec}(\tilde{\mathbf{D}})$, $\mathbf{q} = \mathrm{vec}(\mathbf{Q})$, and $\tilde{\mathbf{n}} = \mathrm{vec}(\tilde{\mathbf{N}})$. The covariance matrix of the noise $\tilde{\mathbf{n}}$ in (21) is denoted by

$$\mathbf{R}_{\tilde{\mathbf{n}}} = (\mathbf{U}_N^T \otimes \mathbf{U}_M^T)\mathbf{R}_{\mathbf{n}}(\mathbf{U}_N \otimes \mathbf{U}_M) \in \mathbb{R}^{K\times K}.$$

We will estimate $\mathbf{Q}$ based on a (weighted) LS formulation with a *unitary* constraint, as given by

$$\arg\min_{\mathbf{Q}} \|\mathbf{R}_{\tilde{\mathbf{n}}}^{-1/2}(\tilde{\mathbf{d}} - (\bar{\mathbf{C}}^T \otimes \bar{\mathbf{A}})\mathbf{q})\|_2^2 \qquad (22a)$$

$$\text{s.t.}\quad \mathbf{q} = \mathrm{vec}(\mathbf{Q}), \mathbf{Q}^T\mathbf{Q} = \mathbf{I}_3. \qquad (22b)$$

The optimization problem in (22) is *nonconvex* due to the quadratic equality constraint, and does not generally admit a known closed-form solution. However, such optimization problems can be solved iteratively as will be discussed later on. Before presenting the iterative algorithm, we will first look at a simplified version of (22).

1) Simplified Unitarily Constrained LS (SCLS) Estimator: The optimization problem in (22) can be simplified and brought to the standard form of an *orthogonal Procrustes problem* (OPP) with a non-iterative known solution. The OPP is generally used to compute rotations between subspaces.

Assuming that $\bar{\mathbf{A}}$ has full column-rank (this can be ensured with optimal anchor placement [21]), and multiplying both sides of (20) with $\bar{\mathbf{A}}^{\dagger}$, we obtain

$$\check{\mathbf{D}} = \mathbf{Q}\bar{\mathbf{C}} + \check{\mathbf{N}}, \qquad (23)$$

where $\check{\mathbf{D}} := \bar{\mathbf{A}}^{\dagger}\tilde{\mathbf{D}}$ and $\check{\mathbf{N}} := \bar{\mathbf{A}}^{\dagger}\tilde{\mathbf{N}}$. The simplified unitarily constrained LS (SCLS) problem is then given as

$$\begin{aligned}\widehat{\mathbf{Q}}_{\mathrm{SCLS}} = \arg\min_{\mathbf{Q}} &\quad \|\check{\mathbf{D}} - \mathbf{Q}\bar{\mathbf{C}}\|_F^2\\ \text{s.t.} &\quad \mathbf{Q}^T\mathbf{Q} = \mathbf{I}_3. \qquad (24)\end{aligned}$$

The SCLS estimator in (24) is *suboptimal* for the original problem in (22) due to the colored noise $\check{\mathbf{N}}$ in (23).

Theorem 1 (Solution to the SCLS Problem): The constrained LS problem in (24) admits a non-iterative known solution given by $\widehat{\mathbf{Q}}_{\mathrm{SCLS}} = \mathbf{V}\mathbf{U}^T$, where $\mathbf{V}$ and $\mathbf{U}$ are obtained from the singular value decomposition (SVD) of $\check{\mathbf{D}}\bar{\mathbf{C}}^T =: \mathbf{V}\boldsymbol{\Sigma}\mathbf{U}^T$ in which matrices $\mathbf{V} \in \mathbb{R}^{3\times3}$, $\mathbf{U} \in \mathbb{R}^{3\times3}$ are unitary, and $\boldsymbol{\Sigma} \in \mathbb{R}^{3\times3}$ is diagonal. The obtained solution is unique if and only if $\check{\mathbf{D}}\bar{\mathbf{C}}^T$ is non-singular.

Proof: See [22, pg. 601]. □

Remark 1 (Alternative SCLS Formulation): Instead of pseudo inverting $\bar{\mathbf{A}}$ in (20) to arrive at (23), we can alternatively pseudo-invert $\bar{\mathbf{C}}$ in (20) to arrive at another OPP given by

$$\begin{aligned}\widehat{\mathbf{Q}}_{\text{A-SCLS}} = \arg\min_{\mathbf{Q}} &\|\breve{\mathbf{D}} - \bar{\mathbf{A}}\mathbf{Q}\|_F^2\\ \text{s.t.} &\quad \mathbf{Q}^T\mathbf{Q} = \mathbf{I}_3, \qquad (25)\end{aligned}$$

where $\breve{\mathbf{D}} := \tilde{\mathbf{D}}\bar{\mathbf{C}}^{\dagger}$. The OPP in (25) has a closed-form solution $\widehat{\mathbf{Q}}_{\text{A-SCLS}} = \mathbf{U}\mathbf{V}^T$, where the unitary matrices $\mathbf{U} \in \mathbb{R}^{3\times3}$ and $\mathbf{V} \in \mathbb{R}^{3\times3}$ are obtained from the SVD of $\bar{\mathbf{A}}^T\breve{\mathbf{D}} =: \mathbf{U}\boldsymbol{\Sigma}\mathbf{V}^T$.

Pseudo inverting $\bar{\mathbf{C}}$ can often assure better conditioning as the topology matrix is usually designed at the factory. However, the alternative SCLS formulation in (25) cannot be used in case of perturbations on the sensor positions, which is discussed in Section V. Hence, from now on we will not consider the approach in Remark 1.

Subsequently, the SCLS estimate of the translation $\mathbf{t}$ can be computed using $\widehat{\mathbf{Q}}_{\mathrm{SCLS}}$ obtained by solving (24). We can write (14) equivalently as

$$\bar{\mathbf{d}} = \left[(\mathbf{C}^T \otimes \bar{\mathbf{A}}) \mid (1_N \otimes \bar{\mathbf{A}})\right] \begin{bmatrix}\mathbf{q}\\ \mathbf{t}\end{bmatrix} + \bar{\mathbf{n}}, \tag{26}$$

where $(\mathbf{C}^T \otimes \bar{\mathbf{A}}) \in \mathbb{R}^{(M-1)N\times 9}$, and $(\mathbf{1}_N \otimes \bar{\mathbf{A}}) \in \mathbb{R}^{(M-1)N\times 3}$. Substituting $\widehat{\mathbf{q}}_{\mathrm{SCLS}} := \mathrm{vec}(\widehat{\mathbf{Q}}_{\mathrm{SCLS}})$ in the above model, and moving the knowns to the left side, we get the following linear model

$$\bar{\mathbf{d}} - (\mathbf{C}^T \otimes \bar{\mathbf{A}})\widehat{\mathbf{q}}_{\mathrm{SCLS}} = (\mathbf{1}_N \otimes \bar{\mathbf{A}})\mathbf{t} + \bar{\mathbf{n}}.$$

The SCLS estimate for the translations is given by the following LS estimate

$$\begin{aligned}\widehat{\mathbf{t}}_{\mathrm{SCLS}} &= \arg\min_{\mathbf{t}} \|\bar{\mathbf{d}} - (\mathbf{C}^T \otimes \bar{\mathbf{A}})\widehat{\mathbf{q}}_{\mathrm{SCLS}} - (\mathbf{1}_N \otimes \bar{\mathbf{A}})\mathbf{t}\|_2^2 \\ &= (\mathbf{1}_N \otimes \bar{\mathbf{A}})^{\dagger}(\bar{\mathbf{d}} - (\mathbf{C}^T \otimes \bar{\mathbf{A}})\widehat{\mathbf{q}}_{\mathrm{SCLS}}). \end{aligned}\tag{27}$$

Since we solve the SCLS estimates in an unweighted LS sense, we need not compute the related noise covariance estimates.

2) Unitarily Constrained LS (CLS) Estimator: The CLS estimates are obtained by solving the optimization problem that was introduced earlier in (22), which we recall as

$$\widehat{\mathbf{Q}}_{\mathrm{CLS}} = \arg\min_{\mathbf{Q}} \left\|\mathbf{R}_{\tilde{\mathbf{n}}}^{-1/2}(\tilde{\mathbf{d}} - (\bar{\mathbf{C}}^T \otimes \bar{\mathbf{A}})\mathbf{q})\right\|_2^2 \tag{28a}$$

$$\text{s.t.} \quad \mathbf{q} = \mathrm{vec}(\mathbf{Q}),\ \mathbf{Q}^T\mathbf{Q} = \mathbf{I}_3. \tag{28b}$$

The optimization problem in (28) is a generalization of the OPP, and is sometimes also referred to as the *weighted orthogonal Procrustes problem* (WOPP) [23]. Unlike the OPP of (24), which has a closed-form analytical solution, the optimization problem (28) does not admit a closed-form solution. However, it can be solved using iterative methods based on either Gauss-Newton's method, Newton's method [23], or steepest descent [24]. In this paper, we restrict ourselves to Gauss-Newton's method for solving (28) because of the availability of a good initial value (e.g., the closed-form solution from Theorem 1) for the iterative algorithm.

The optimization problem in (28) is a LS problem on the Stiefel manifold. To simplify the notations we write (28) in a more general form:

$$\begin{aligned}&\arg\min_{\mathbf{Q}} \|\mathbf{z} - \mathbf{L}\mathrm{vec}(\mathbf{Q})\|_2^2 \\ &\text{s.t.} \quad \mathbf{Q} \in \mathcal{V}_{3,3},\end{aligned}\tag{29}$$

and for solving (28) we use

$$\begin{aligned}&\mathbf{z} := \mathbf{R}_{\tilde{\mathbf{n}}}^{-1/2}\tilde{\mathbf{d}} \in \mathbb{R}^{K\times 1}, \\ \text{and} \quad &\mathbf{L} := \mathbf{R}_{\tilde{\mathbf{n}}}^{-1/2}(\bar{\mathbf{C}}^T \otimes \bar{\mathbf{A}}) \in \mathbb{R}^{K\times 9}.\end{aligned}\tag{30}$$

The algorithm is derived in Appendix B, and it is summarized as Algorithm 1. A more profound treatment on WOPP is found in [23].

Algorithm 1: CLS based on Gauss-Newton's method.

1. **Compute initial value** $\mathbf{Q}_0 := \widehat{\mathbf{Q}}_{\mathrm{SCLS}}$,
2. **initialize** $\mathbf{L}$, $\mathbf{z}$, iteration counter $k = 0$, ε, and ε_0.
3. **while** $\varepsilon_k > \varepsilon$
4. **compute** $\mathbf{J}$ using (48)
5. **compute** a *Gauss-Newton* step
   $$\mathbf{x}_k = (\mathbf{J}^T\mathbf{J})^{-1}\mathbf{J}^T(\mathbf{z} - \mathbf{L}\mathrm{vec}(\mathbf{Q}_k))$$
6. **compute** the optimal step-length α_k using (50).
7. **update** $\mathbf{Q}_{k+1} = \mathbf{Q}_k\mathbf{\Omega}(\alpha_k\mathbf{x}_k)$, where $\mathbf{\Omega}(\cdot)$ is defined in (46).
8. **increment** $k = k + 1$.
9. **compute** $\varepsilon_{k+1} = \frac{\|\mathbf{J}^T(\mathbf{z}-\mathbf{L}\mathrm{vec}(\mathbf{Q}_k))\|_2}{\|\mathbf{J}\|_F\|\mathbf{z}-\mathbf{L}\mathrm{vec}(\mathbf{Q}_k)\|_2}$.
10. **end while.**

As before, the estimate for the translation $\mathbf{t}$ can then be computed using $\widehat{\mathbf{q}}_{\mathrm{CLS}} := \mathrm{vec}(\widehat{\mathbf{Q}}_{\mathrm{CLS}})$ in (26). The CLS estimate for the translation is given by the following (weighted) LS estimate

$$\begin{aligned}\widehat{\mathbf{t}}_{\mathrm{CLS}} &= \arg\min_{\mathbf{t}} \|\bar{\mathbf{d}}' - \mathbf{R}_{\bar{\mathbf{n}}}^{-1/2}((\mathbf{C}^T \otimes \bar{\mathbf{A}})\widehat{\mathbf{q}}_{\mathrm{SCLS}} + (\mathbf{1}_N \otimes \bar{\mathbf{A}})\mathbf{t})\|_2^2 \\ &= (\mathbf{R}_{\bar{\mathbf{n}}}^{-1/2}(\mathbf{1}_N \otimes \bar{\mathbf{A}}))^{\dagger}(\bar{\mathbf{d}}' - \mathbf{R}_{\bar{\mathbf{n}}}^{-1/2}(\mathbf{C}^T \otimes \bar{\mathbf{A}})\widehat{\mathbf{q}}_{\mathrm{CLS}}).\end{aligned}$$

D. Topology-Aware (TA) Localization

A complementary by-product of the rigid body localization is the *topology-aware* localization. In this case, the position and orientation estimation is not the main interest, but the absolute position of each sensor node has to be estimated, given that the sensors follow a certain topology. This latter information can be used as a constraint for estimating the sensor positions rather than estimating them separately. For the rigidity constraint, using $\widehat{\mathbf{Q}}$ and $\widehat{\mathbf{t}}$ obtained from either the SCLS or CLS estimator, we can then compute the absolute positions of each sensor on the rigid body as

$$\widehat{\mathbf{S}}_{\mathrm{TA}} = \widehat{\mathbf{Q}}\mathbf{C} + \widehat{\mathbf{t}}\mathbf{1}_N^T. \tag{31}$$

IV. Unitarily Constrained Cramér–Rao Bound

Suppose we want to estimate the unknown vector $\boldsymbol{\theta} = [\mathbf{q}_1^T, \mathbf{q}_2^T, \mathbf{q}_3^T, \mathbf{t}^T]^T \in \mathbb{R}^{12\times 1}$ from the range measurements y_{mn} corrupted by independent noise $v_{mn} \sim \mathcal{N}(0, \sigma_{mn}^2)$ for $n = 1, 2, \ldots, N$, and $m = 1, 2, \ldots, M$, where the observations follow the non-linear model (3). We can compute the CRB for any unbiased estimator of $\boldsymbol{\theta}$ as described next.

A. Unconstrained CRB

The covariance matrix of any unbiased estimate of the parameter vector $\boldsymbol{\theta}$ satisfies [25]

$$\mathbb{E}\{(\widehat{\boldsymbol{\theta}} - \boldsymbol{\theta})(\widehat{\boldsymbol{\theta}} - \boldsymbol{\theta})^T\} \geq \mathbf{C}_{\mathrm{CRB}} = \mathbf{F}^{-1},$$

where the Fisher information matrix (FIM) $\mathbf{F}$ is given by

$$\mathbf{F} = \sum_{m=1}^{M}\sum_{n=1}^{N}\mathbb{E}\left\{\left(\frac{\partial \ln p(y_{mn};\boldsymbol{\theta})}{\partial\boldsymbol{\theta}}\right)\left(\frac{\partial \ln p(y_{mn};\boldsymbol{\theta})}{\partial\boldsymbol{\theta}}\right)^T\right\}.$$

This is the *Cramér–Rao bound theorem* and $\mathbf{C}_{\mathrm{CRB}}$ is the Cramér–Rao lower bound (CRB). Let us define $\mathbf{c}_{\mathrm{e},m} = [\mathbf{c}_m^T, 1]^T \in \mathbb{R}^4$ for $m = 1, 2, \ldots, M$. The computation of the CRB for observations with Gaussian likelihoods is straightforward, and is given as (32) at the bottom of the page.

B. Constrained CRB

The FIM in (32), does not take into account the unitary constraint on the matrix $\mathbf{Q}$, i.e., $\mathbf{Q}^T\mathbf{Q} = \mathbf{I}_3$. Generally, if the parameter vector $\boldsymbol{\theta}$ is subject to some P continuously differentiable (non-redundant) constraints $\mathbf{h}(\boldsymbol{\theta}) = \mathbf{0}$, then with these constraints, the resulting constrained CRB is lower than the unconstrained CRB. In [26], it is shown that the constrained CRB (CCRB) has the form

$$\mathbf{C}_{\mathrm{CCRB}}(\boldsymbol{\theta}) = \mathbb{E}\{(\widehat{\boldsymbol{\theta}}-\boldsymbol{\theta})(\widehat{\boldsymbol{\theta}}-\boldsymbol{\theta})^T\} \geq \mathbf{M}(\mathbf{M}^T\mathbf{F}\mathbf{M})^{-1}\mathbf{M}^T, \tag{33}$$

where $\mathbf{F}$ is the FIM for the unconstrained estimation problem as in (32), and an isometry matrix $\mathbf{M} \in \mathbb{R}^{12\times(12-P)}$ is obtained by collecting orthonormal basis vectors of the null-space of the gradient matrix

$$\mathbf{G}(\boldsymbol{\theta}) = \frac{\partial \mathbf{h}(\boldsymbol{\theta})}{\partial \boldsymbol{\theta}^T} \in \mathbb{R}^{P\times 12}.$$

The non-redundant constraints ensure that the matrix $\mathbf{G}(\boldsymbol{\theta})$ is full row-rank, and implies

$$\mathbf{G}(\boldsymbol{\theta})\mathbf{M} = \mathbf{0}$$

while $\mathbf{M}^T\mathbf{M} = \mathbf{I}_{12-P}$. For the unitarily constrained CRB (CCRB) denoted by $\mathbf{C}_{\mathrm{CCRB}}(\boldsymbol{\theta})$, we have to consider the unitary constraint $\mathbf{Q}^T\mathbf{Q} = \mathbf{I}_3$, which can be expressed by the following $P = 6$ non-redundant constraints

$$\begin{aligned}\mathbf{h}(\boldsymbol{\theta}) = [&\mathbf{q}_1^T\mathbf{q}_1 - 1, \mathbf{q}_2^T\mathbf{q}_1, \mathbf{q}_3^T\mathbf{q}_1, \mathbf{q}_2^T\mathbf{q}_2 - 1,\\ &\mathbf{q}_3^T\mathbf{q}_2, \mathbf{q}_3^T\mathbf{q}_3 - 1]^T = \mathbf{0}_6 \in \mathbb{R}^{6\times 1},\end{aligned} \tag{34}$$

where the symmetric redundant constraints are discarded. The gradient matrix for the constraints in (34) can be computed as follows

$$\mathbf{G}(\boldsymbol{\theta}) = \frac{\partial \mathbf{h}(\boldsymbol{\theta})}{\partial \boldsymbol{\theta}^T}$$

$$= \begin{bmatrix} 2\mathbf{q}_1^T & \mathbf{0}_3^T & \mathbf{0}_3^T & \mathbf{0}_3^T \\ \mathbf{q}_2^T & \mathbf{q}_1^T & \mathbf{0}_3^T & \mathbf{0}_3^T \\ \mathbf{q}_3^T & \mathbf{0}_3^T & \mathbf{q}_1^T & \mathbf{0}_3^T \\ \mathbf{0}_3^T & 2\mathbf{q}_2^T & \mathbf{0}_3^T & \mathbf{0}_3^T \\ \mathbf{0}_3^T & \mathbf{q}_3^T & \mathbf{q}_2^T & \mathbf{0}_3^T \\ \mathbf{0}_3^T & \mathbf{0}_3^T & 2\mathbf{q}_3^T & \mathbf{0}_3^T \end{bmatrix} \in \mathbb{R}^{6\times 12}.$$

An orthonormal basis of the null-space of the gradient matrix is finally given by

$$\mathbf{M} = \frac{1}{\sqrt{2}}\left[\begin{array}{ccc|c} -\mathbf{q}_3 & \mathbf{0}_3 & \mathbf{q}_2 & \\ \mathbf{0}_3 & -\mathbf{q}_3 & -\mathbf{q}_1 & \mathbf{0}_{3\times 3} \\ \mathbf{q}_1 & \mathbf{q}_2 & \mathbf{0}_3 & \\ \hline & \mathbf{0}_{3\times 3} & & \sqrt{2}\,\mathbf{I}_3 \end{array}\right].$$

The CCRB for TA-localization can be easily derived from $\mathbf{C}_{\mathrm{CCRB}}(\boldsymbol{\theta})$ using the transformation of parameters [25].

Theorem 2 (Biased Estimator): An unbiased constrained estimator for $\mathbf{Q}$ does not exist, except for the noiseless case.

Proof: See Appendix C. □

Due to Theorem 2, the mean-squared-error (MSE) of any unitarily constrained estimator will be lower than the CCRB for high noise levels. However, at low noise levels, the bias tends to zero, and the CCRB gives a good lower bound on the MSE of the unitarily constrained estimators.

V. Unitarily Constrained Total-Least-Squares

In the previous section, we assumed that the position of the sensors on the rigid body in the reference frame, i.e., the matrix $\mathbf{C}$, is accurately known. In practice, there is no reason to believe that errors are restricted only to the range measurements and there are no perturbations on the initial sensor positions. Such perturbations can be introduced for instance during fabrication or if the body is not entirely rigid (e.g., wing flexing of an aircraft).

Let us assume that the position of the nth sensor in the reference frame $\mathbf{c}_n$ is noisy, and let us denote the perturbation on $\mathbf{c}_n$ by $\mathbf{e}_n$, and the perturbation on $\mathbf{C} = [\mathbf{c}_1, \mathbf{c}_2, \ldots, \mathbf{c}_N]$ by $\mathbf{E} = [\mathbf{e}_1, \mathbf{e}_2, \ldots, \mathbf{e}_N] \in \mathbb{R}^{3\times N}$. The covariance matrix of the perturbation $\mathbf{e} = \mathrm{vec}(\mathbf{E})$ is denoted by $\mathbf{R}_{\mathbf{e}} = \sigma_{\mathrm{e}}^2\mathbf{I}_{3N}$. In other words, we assume that the perturbations $\mathbf{e}_n, n = 1, 2, \ldots, N$, are a sequence of independent and identically distributed (i.i.d.) random vectors. To account for such errors in the model, we next propose total-least-squares (TLS) estimators again with unitary constraints.

A. Simplified Unitarily Constrained TLS (SCTLS) Estimator

Taking the perturbations on the known topology into account, the data model in (20) will be modified as

$$\tilde{\mathbf{D}} = \bar{\mathbf{A}}\mathbf{Q}(\bar{\mathbf{C}} + \bar{\mathbf{E}}) + \tilde{\mathbf{N}},$$

$$\mathbf{F}(\boldsymbol{\theta}) = \sum_{m=1}^{M}\sum_{n=1}^{N}\frac{(\mathbf{c}_{\mathrm{e},m}^T \otimes \mathbf{I}_3)(\mathbf{a}_m - (\mathbf{Q}\mathbf{c}_n + \mathbf{t}))(\mathbf{a}_m - (\mathbf{Q}\mathbf{c}_n + \mathbf{t}))^T(\mathbf{c}_{\mathrm{e},m} \otimes \mathbf{I}_3)}{\sigma_{mn}^2\|\mathbf{a}_m - (\mathbf{Q}\mathbf{c}_n + \mathbf{t})\|_2^2} \in \mathbb{R}^{12\times 12}. \tag{32}$$

where $\bar{\mathbf{E}} = \mathbf{E}\mathbf{U}_N$. Multiplying both sides of the above equation with $\bar{\mathbf{A}}^\dagger$, we get

$$\check{\mathbf{D}} = \mathbf{Q}(\bar{\mathbf{C}} + \bar{\mathbf{E}}) + \check{\mathbf{N}}. \tag{35}$$

The solution to the data model in (35) admits a classical TLS formulation, but with a unitary constraint. The SCTLS optimization problem is given by

$$\widehat{\mathbf{Q}}_{\mathrm{SCTLS}} = \arg\min_{\mathbf{Q}} \quad \|\bar{\mathbf{E}}\|_F^2 + \|\check{\mathbf{N}}\|_F^2 \\ \text{s.t.} \quad \check{\mathbf{D}} = \mathbf{Q}(\bar{\mathbf{C}} + \bar{\mathbf{E}}) + \check{\mathbf{N}}, \text{ and } \mathbf{Q}^T\mathbf{Q} = \mathbf{I}_3. \tag{36}$$

Similar to SCLS, the optimization problem in (36) admits a known closed-form solution which makes it simplified compared to the weighted problem discussed in the next section. Also, the noise $\check{\mathbf{N}}$ in (35) is not white leading to a suboptimal solution.

Theorem 3 (Solution to SCTLS): The SCTLS problem in (36) has the same solution as the simplified unitarily constrained LS problem, i.e., $\widehat{\mathbf{Q}}_{\mathrm{SCTLS}} = \widehat{\mathbf{Q}}_{\mathrm{SCLS}}$.

Proof: See Appendix D. □

We next estimate the translation vector $\mathbf{t}$. Taking the perturbations into account, we can modify the model in (13) as

$$\bar{\mathbf{D}} = \bar{\mathbf{A}}\mathbf{Q}\mathbf{C} + \bar{\mathbf{A}}\mathbf{t}\mathbf{1}_N^T + \bar{\mathbf{A}}\mathbf{Q}\mathbf{E} + \bar{\mathbf{N}},$$

which can be vectorized and further simplified to

$$\bar{\mathbf{d}} - (\mathbf{C}^T \otimes \bar{\mathbf{A}})\mathbf{q} = (\mathbf{1}_N \otimes \bar{\mathbf{A}})\mathbf{t} + \overbrace{(\mathbf{I} \otimes \bar{\mathbf{A}}\mathbf{Q})\mathbf{e} + \bar{\mathbf{n}}}^{\boldsymbol{\nu} \in \mathbb{R}^{(M-1)N}}. \tag{37}$$

Using $\widehat{\mathbf{q}}_{\mathrm{SCLS}}$ in the above model, the SCTLS estimator for the translation taking perturbations into account, is then given by the following (unweighted) LS problem

$$\widehat{\mathbf{t}}_{\mathrm{SCLS}} = \arg\min_{\mathbf{t}} \|\bar{\mathbf{d}} - (\mathbf{C}^T \otimes \bar{\mathbf{A}})\widehat{\mathbf{q}}_{\mathrm{SCLS}} - (\mathbf{1}_N \otimes \bar{\mathbf{A}})\mathbf{t}\|_2^2 \\ = (\mathbf{1}_N \otimes \bar{\mathbf{A}})^\dagger(\bar{\mathbf{d}} - (\mathbf{C}^T \otimes \bar{\mathbf{A}})\widehat{\mathbf{q}}_{\mathrm{SCLS}}).$$

The algorithms to compute the SCTLS estimates are the same as that of the SCLS estimator. As before, we solve SCTLS in an unweighted LS sense, therefore, we need not estimate the related noise covariance matrix for whitening.

B. Unitarily Constrained TLS (CTLS) Estimator

Similar to the CLS formulation, the TLS estimator can be derived without pseudo inverting the matrix $\bar{\mathbf{A}}$. The data model in (20) taking into account the perturbations on the known sensor topology is then given by

$$\tilde{\mathbf{D}} = \bar{\mathbf{A}}\mathbf{Q}(\bar{\mathbf{C}} + \bar{\mathbf{E}}) + \tilde{\mathbf{N}}, \tag{38}$$

which can be further vectorized as

$$\tilde{\mathbf{d}} = (\mathbf{I}_{3(N-1)} \otimes \bar{\mathbf{A}}\mathbf{Q})\bar{\mathbf{c}} + (\mathbf{I}_{3(N-1)} \otimes \bar{\mathbf{A}}\mathbf{Q})\bar{\mathbf{e}} + \tilde{\mathbf{n}}, \tag{39}$$

where $\bar{\mathbf{c}} = \mathrm{vec}(\bar{\mathbf{C}}) \in \mathbb{R}^{3(N-1)}$, and $\bar{\mathbf{e}} = \mathrm{vec}(\bar{\mathbf{E}}) \in \mathbb{R}^{3(N-1)}$.

Assuming that the pre-whitening matrix takes the block diagonal form $\mathbf{R}_{\boldsymbol{\epsilon}}^{-1/2} := \mathrm{diag}(\sigma_{\mathrm{e}}^{-1}\mathbf{I}_{3(N-1)}, \mathbf{R}_{\tilde{\mathbf{n}}}^{-1/2})$ with $\boldsymbol{\epsilon} = [\bar{\mathbf{e}}^T, \tilde{\mathbf{n}}^T]^T$, the CTLS optimization problem is given by

$$\arg\min_{\mathbf{Q}} \quad \|\sigma_{\mathrm{e}}^{-1}\bar{\mathbf{e}}\|_2^2 + \|\mathbf{R}_{\tilde{\mathbf{n}}}^{-1/2}\tilde{\mathbf{n}}\|_2^2 \\ \text{s.t.} \quad \tilde{\mathbf{D}} = \bar{\mathbf{A}}\mathbf{Q}(\bar{\mathbf{C}} + \bar{\mathbf{E}}) + \tilde{\mathbf{N}}, \\ \bar{\mathbf{e}} = \mathrm{vec}(\bar{\mathbf{E}}), \quad \tilde{\mathbf{n}} = \mathrm{vec}(\tilde{\mathbf{N}}), \\ \mathbf{Q}^T\mathbf{Q} = \mathbf{I}_3. \tag{40}$$

Theorem 4 (Solution to CTLS): Assuming that the covariance matrix of the perturbation vector is a scaled identity matrix, the unitarily constrained TLS problem in (40) has the same solution as a specifically weighted CLS, i.e., it is the solution to

$$\widehat{\mathbf{Q}}_{\mathrm{CTLS}} = \arg\min_{\mathbf{Q}} \|\boldsymbol{\Lambda}^{1/2}(\tilde{\mathbf{d}} - (\bar{\mathbf{C}}^T \otimes \bar{\mathbf{A}})\mathbf{q})\|_2^2 \\ \text{s.t.} \quad \mathbf{Q}^T\mathbf{Q} = \mathbf{I}_3, \tag{41}$$

where matrix $(\bar{\mathbf{C}}^T \otimes \bar{\mathbf{A}}) \in \mathbb{R}^{K \times 9}$ was defined earlier, and $\boldsymbol{\Lambda} \in \mathbb{R}^{K \times K}$ is the specific weighting matrix defined in (57).

Proof: See Appendix E. □

The optimization problem (41) does not have a closed-form solution, and has to be solved iteratively using for instance Gauss-Newton's method (summarized in Algorithm 1) with

$$\mathbf{z} := \boldsymbol{\Lambda}^{1/2}\tilde{\mathbf{d}} \in \mathbb{R}^{K \times 1}, \\ \text{and} \qquad \mathbf{L} := \boldsymbol{\Lambda}^{1/2}(\bar{\mathbf{C}}^T \otimes \bar{\mathbf{A}}) \in \mathbb{R}^{K \times 9}. \tag{42}$$

The CTLS estimates for the translations can be computed similar to SCTLS as earlier, however, for CTLS we first pre-whiten the noise. The covariance of the noise $\boldsymbol{\nu}$ in (37) is denoted by an $(M-1)N \times (M-1)N$ matrix $\mathbf{R}_{\boldsymbol{\nu}} := \sigma_{\mathrm{e}}^2(\mathbf{I} \otimes \bar{\mathbf{A}}\bar{\mathbf{A}}^T) + \mathbf{R}_{\bar{\mathbf{n}}}$. We can then use a weighted LS estimator to estimate the translations accounting for the perturbations. The CTLS translation estimates are given by

$$\widehat{\mathbf{t}}_{\mathrm{CTLS}} = \arg\min_{\mathbf{t}} \|\mathbf{R}_{\boldsymbol{\nu}}^{-1/2}(\bar{\mathbf{d}} - (\mathbf{C}^T \otimes \bar{\mathbf{A}})\widehat{\mathbf{q}}_{\mathrm{CTLS}} - (\mathbf{1}_N \otimes \bar{\mathbf{A}})\mathbf{t})\|_2^2 \\ = (\mathbf{R}_{\boldsymbol{\nu}}^{-1/2}(\mathbf{1}_N \otimes \bar{\mathbf{A}}))^\dagger \mathbf{R}_{\boldsymbol{\nu}}^{-1/2}(\bar{\mathbf{d}} - (\mathbf{C}^T \otimes \bar{\mathbf{A}})\widehat{\mathbf{q}}_{\mathrm{CTLS}}).$$

VI. Simulation Results

We consider $N = 5$ sensors mounted on the vertices of a rigid body (rectangle based pyramid as in Fig. 1) with

$$\mathbf{C} = \begin{bmatrix} 0.5 & 1.5 & 1.5 & 0.5 & 1 \\ 0 & 0 & 1.5 & 1.5 & 1 \\ 0 & 0 & 0 & 0 & 1 \end{bmatrix} \text{ m},$$

and $M = 4$ anchors fixed at location

$$\mathbf{A} = \begin{bmatrix} 0 & 100 & 0 & 100 \\ 100 & 100 & 0 & 0 \\ 0 & 100 & 100 & 0 \end{bmatrix} \text{ m}.$$

Let us define a function $\mathcal{R}(\cdot) : \mathbb{R}^3 \to \mathcal{V}_{3,3}$ that maps angles in degrees along each dimension into a rotation matrix, and its inverse $\mathcal{R}^{-1}(\cdot) : \mathcal{V}_{3,3} \rightarrow \mathbb{R}^3$ which maps a rotation matrix into corresponding angles in degrees (see [27] for details on converting angles to a rotation matrix and vice versa). Collecting the angles in a 3×1 vector $\boldsymbol{\phi} = [20, -25, 10]^T$ deg, the rotation matrix is then generated according to $\mathbf{Q} = \mathcal{R}(\boldsymbol{\phi})$. We use a translation vector $\mathbf{t} = [15, 5, 10]^T$ m. The simulations are averaged over $N_{\rm exp} = 1000$ independent Monte-Carlo experiments.

The performance of the proposed estimators is analyzed in terms of the root-mean-squared-error (RMSE) of the estimates of $\mathbf{Q}$, $\boldsymbol{\phi}$, and $\mathbf{t}$, and are respectively given as

$$\mathrm{RMSE}(\mathbf{Q}) = \left(\frac{1}{N_{\rm exp}} \sum_{n=1}^{N_{\rm exp}} \|\mathbf{Q} - \widehat{\mathbf{Q}}^{(n)}\|_F^2 \right)^{1/2},$$
$$\mathrm{RMSE}(\boldsymbol{\phi}) = \left(\frac{1}{N_{\rm exp}} \sum_{n=1}^{N_{\rm exp}} \|\boldsymbol{\phi} - \mathcal{R}^{-1}(\widehat{\mathbf{Q}}^{(n)})\|_2^2 \right)^{1/2} \text{deg},$$
$$\mathrm{RMSE}(\mathbf{t}) = \left(\frac{1}{N_{\rm exp}} \sum_{n=1}^{N_{\rm exp}} \|\mathbf{t} - \widehat{\mathbf{t}}^{(n)}\|_2^2 \right)^{1/2} \text{m},$$

where $\widehat{\mathbf{Q}}^{(n)}$ and $\widehat{\mathbf{t}}^{(n)}$ denote the estimates during the nth Monte-Carlo experiment. Since the rotation matrix estimated using the unconstrained LS estimator is not a valid rotation matrix, we first project it onto $\mathcal{V}_{3,3}$ using (51) before converting it into corresponding angles.

We use the same noise variance for all the range measurements, i.e., $\sigma_{mn} = \sigma$ m for $m = 1, 2, \ldots, M$, and $n = 1, 2, \ldots, N$. The covariance matrix of the noise $\mathbf{n}$, i.e., (see Appendix A)

$$\mathbf{R}_{\mathbf{n}} = \mathrm{diag}(2\boldsymbol{\rho})\mathbf{R}_{\mathbf{v}}\mathrm{diag}(2\boldsymbol{\rho}) + \mathbf{R}_{\mathbf{v}^{\odot 2}} - \boldsymbol{\mu}\boldsymbol{\mu}^T,$$

depends on the unknown parameter

$$\boldsymbol{\rho} = [\rho_{11}, \rho_{12}, \ldots, \rho_{M1}, \ldots, \rho_{MN}]^T \in \mathbb{R}^{MN}.$$

Hence, to whiten it, we use the noisy range measurements

$$\mathbf{y} = [y_{11}, y_{12}, \ldots, y_{M1}, \ldots, y_{MN}]^T \in \mathbb{R}^{MN}$$

in (3) instead of $\boldsymbol{\rho}$ to compute the estimated covariance matrix

$$\widehat{\mathbf{R}}_{\mathbf{n}} = \mathrm{diag}(2\mathbf{y})\mathbf{R}_{\mathbf{v}}\mathrm{diag}(2\mathbf{y}) + \mathbf{R}_{\mathbf{v}^{\odot 2}} - \boldsymbol{\mu}\boldsymbol{\mu}^T.$$

We use this estimated covariance matrix for pre-whitening the noise. Simulations are provided for different values of the nominal ranging noise σ m.

In Fig. 2, the RMSE of the estimates $\mathbf{Q}$, $\boldsymbol{\phi}$, and $\mathbf{t}$ for different values of σ is shown. The estimators in Fig. 2 are LS based where the topology of the sensors is assumed to be accurately known. Due to Theorem 2, the RMSE of $\mathbf{Q}$ for the constrained estimators is lower than the CCRB at high noise levels. The saturation of the RMSE in Fig. 2(a) for $\sigma > 1$ m follows from the following lemma.

Lemma 1 (Frobenius Norm Induced Distance): For any matrix $\mathbf{Q}_i$ and $\mathbf{Q}_j$, such that, $\mathbf{Q}_i \in \mathcal{V}_{n,n}$ and $\mathbf{Q}_j \in \mathcal{V}_{n,n}$, the Frobenius norm induced distance is always upper bounded by $\sqrt{2n}$, i.e., $\|\mathbf{Q}_i - \mathbf{Q}_j\|_F \leq \sqrt{\|\mathbf{Q}_i\|_F + \|\mathbf{Q}_j\|_F} = \sqrt{2n}$.

However, the CCRB computed using (33) does not saturate in this range as there exists no unbiased estimator for high noise values as discussed in Theorem 2. Fig. 2(b) shows the RMSE in degrees, which gives an insight into how the error on the range measurements translates to the error on the estimated rotations. For the considered scenario, the range error that yields a positioning accuracy of the order of 10 cm also yields an orientation error accuracy of the order of 0.1 deg.

The bias of both the SCLS and CLS estimators is shown in Fig. 2(c), and it can be seen that the bias tends to zero for $\sigma < 0.1$ m (as discussed in Theorem 2), whereas the unconstrained LS is an unbiased estimator. The bias is computed as

$$\mathrm{bias}(\mathbf{Q}) = \|\frac{1}{N_{\rm exp}} \sum_{n=1}^{N_{\rm exp}} \mathrm{vec}(\widehat{\mathbf{Q}}^{(n)}) - \mathrm{vec}(\mathbf{Q})\|_2.$$

We can see a significant (close to an order of magnitude) improvement in the performance of the location estimates when the knowledge of the topology is exploited as compared to the topology-agnostic case (see Fig. 2(d)). The performance of the SCLS estimator is similar (slightly worse) to that of the iterative CLS estimator. The resulting gap between the RMSE and the root-CRB is reasonable, and thus the proposed estimators are robust to the linearization via squaring.

Fig. 3 illustrates the effect of a bad anchor geometry, where we use an ill-conditioned matrix $\mathbf{A}$ with a condition number of 100. The performance of the SCLS estimators (based on pseudo inverting $\bar{\mathbf{A}}$) deteriorates for scenarios with a bad anchor geometry, however, the performance of the CLS estimators is not affected. Nevertheless, if the topology is not subject to perturbations, the solution proposed in Remark 1 can be used for scenarios with a bad anchor geometry, in which a well-conditioned $\mathbf{C}$ can always be designed.

The convergence (i.e., $\varepsilon_k := \frac{\|\mathbf{J}^T(\mathbf{z} - \mathbf{L}\mathrm{vec}(\mathbf{Q}_k))\|_2}{\|\mathbf{J}\|_F \|\mathbf{z} - \mathbf{L}\mathrm{vec}(\mathbf{Q}_k)\|_2}$, where $\mathbf{J}$ defined in (48)) of Gauss-Newton's method with $\sigma = 10^{-2}$ m for the optimal step-size and a fixed step-size is shown in Fig. 4. We can see that it is sufficient to use a fixed step-size $\alpha_k = 1$ at low noise levels. As observed from the simulations, the iterative algorithm requires typically ten or fewer iterations.

In order to analyze the performance of the estimators for the case when the sensor topology is perturbed, we corrupt the sensor coordinates in the reference frame with a zero mean i.i.d. Gaussian random process of standard deviation $\sigma_{\rm e} = 1$ cm. The RMSE of the estimates of $\mathbf{Q}$, $\boldsymbol{\phi}$, and $\mathbf{t}$ using the unconstrained LS, SCLS/SCTLS, CLS and CTLS estimators is shown in Fig. 5. The performance of these estimators is similar to that of the LS-based estimators, except for the error floor, and this is due to the model error (perturbations on the sensor topology). The estimators hit the error floor for lower values of σ as $\sigma_{\rm e}^2$ increases. With an ill-conditioned matrix $\mathbf{A}$, the performance of the SCLS/SCTLS (and the unconstrained LS) estimator is worse than the CLS and CTLS estimators.

VII. CONCLUSIONS

A framework for joint position and orientation estimation of a rigid body based on range measurements is proposed. We refer to this problem as rigid body localization. Sensor nodes can be

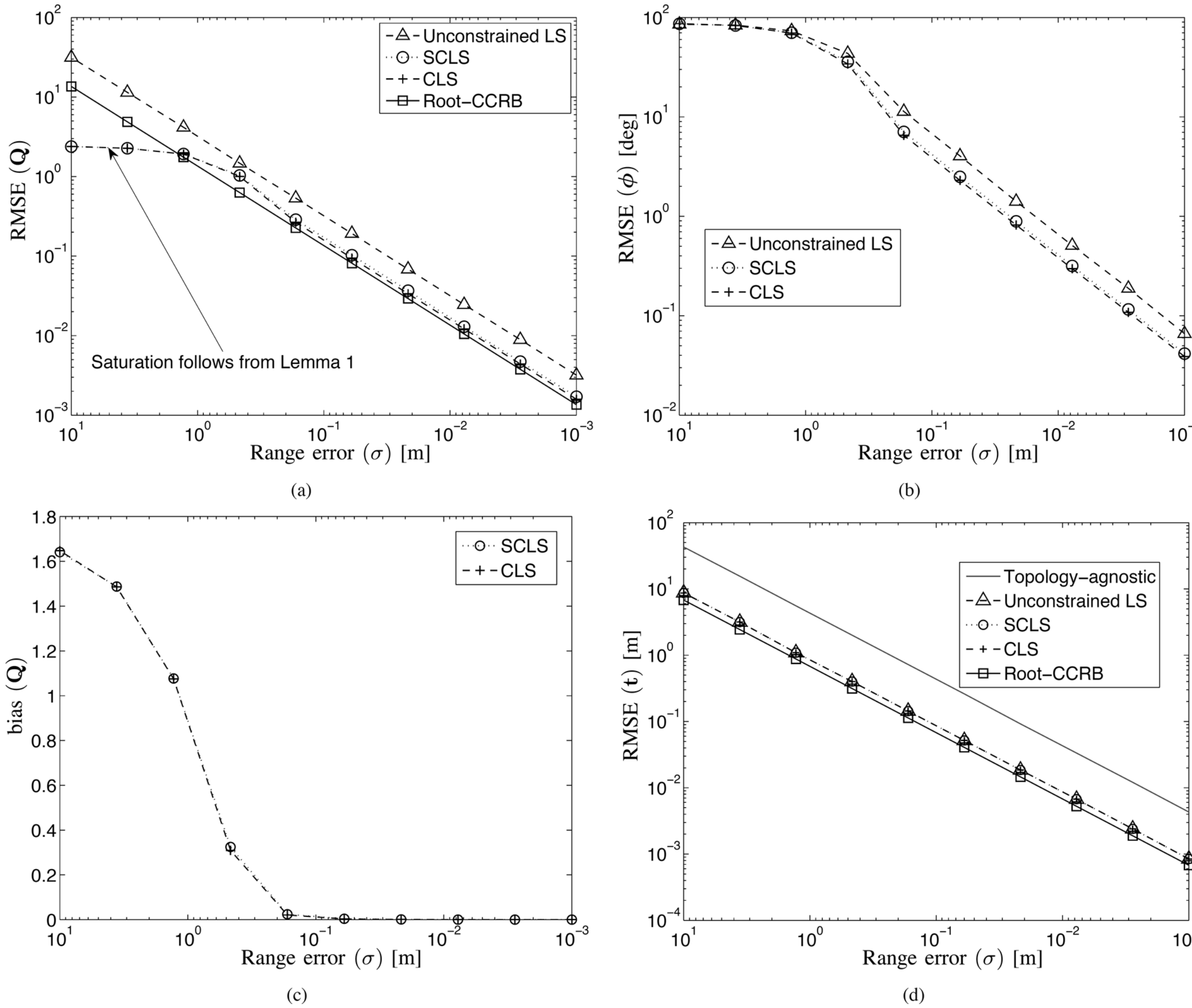

Fig. 2. (a) RMSE of the estimated rotation matrix $\mathbf{Q}$. The RMSE of the constrained estimators is upper bounded as discussed in Remark 1. (b) RMSE in degrees of the estimated rotations. (c) Bias in the SCLS and CLS estimators for $\mathbf{Q}$. Bias tends to zero for low noise variance. (d) RMSE of the estimated translation vector $\mathbf{t}$ along with the solution from the classical LS-based localization.

mounted on the rigid bodies (e.g., satellites, robots) during fabrication at the factory, and the geometry of how these sensors are mounted is known *a priori* up to a certain accuracy. However, the absolute position of the rigid body is not known. The original non-linear problem is linearized via squaring of the range measurements. The squared-range measurements between the anchors and the sensors on the rigid body can then be used to estimate the position and the orientation of the body. The position and orientation of the rigid body is determined by a translation vector and a rotation matrix, respectively. Ignoring the fact that the rotation matrix is unitary, an unconstrained estimator is proposed. A number of unitarily constrained LS estimators is also proposed, all of which solve an optimization problem on the Stiefel manifold. All the proposed estimators are robust to linearization via squaring. For good anchor geometries, the performance of the SCLS estimator with a closed-form solution is already reasonable. The gap between the RMSE and root-CCRB of the SCLS and CLS estimates is negligible, however, the estimators do not achieve the CCRB. In addition to this, constrained TLS estimators that take into account the inaccuracies in the known sensor topology are also proposed.

Appendix A
Derivation of the Covariance Matrix $\mathbf{R_n}$

In this section, we develop the covariance matrix $\mathbf{R_n}$ used for pre-whitening. Modeling the noise on the range measurements v_{mn} as a zero-mean additive white Gaussian process having a variance σ_{mn}^2, we can compute the statistics (up to the second-order) of the zero-mean noise in (6), i.e.,

$$n_{mn} = 2\rho_{mn}v_{mn} + v_{mn}^2 - \sigma_{mn}^2 \tag{43}$$

as

$$\begin{aligned}
&\mathbb{E}\{n_{mn}\} = 0,\\
&\mathbb{E}\{(n_{mn} - \mathbb{E}\{n_{mn}\})^2\} = 4\rho_{mn}^2\sigma_{mn}^2 + 2\sigma_{mn}^4,\\
&\mathbb{E}\{(n_{mn} - \mathbb{E}\{n_{mn}\})(n_{ln} - \mathbb{E}\{n_{ln}\})\} = 0, \quad m \neq l,\\
\text{and}\quad &\mathbb{E}\{(n_{mn} - \mathbb{E}\{n_{mn}\})(n_{ml} - \mathbb{E}\{n_{ml}\})\} = 0, \quad n \neq l,
\end{aligned}$$

where we use the fact that, if $v_{mn} \sim \mathcal{N}(0, \sigma_{mn}^2)$ then $\mathbb{E}\{v_{mn}^4\} = 3\sigma_{mn}^4$ and $\mathbb{E}\{v_{mn}^3\} = 0$. Collecting $\rho_{mn}, m = 1, 2, \ldots, M; n = 1, 2, \ldots, N$, in the vector

$$\boldsymbol{\rho} = [\rho_{11}, \rho_{12}, \ldots, \rho_{M1}, \ldots, \rho_{MN}]^T \in \mathbb{R}^{MN},$$

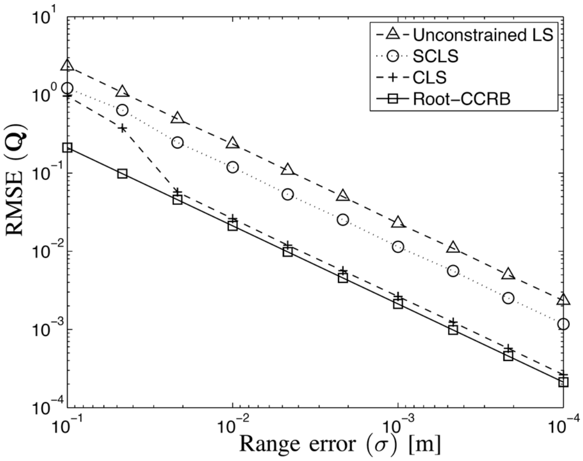

(a)

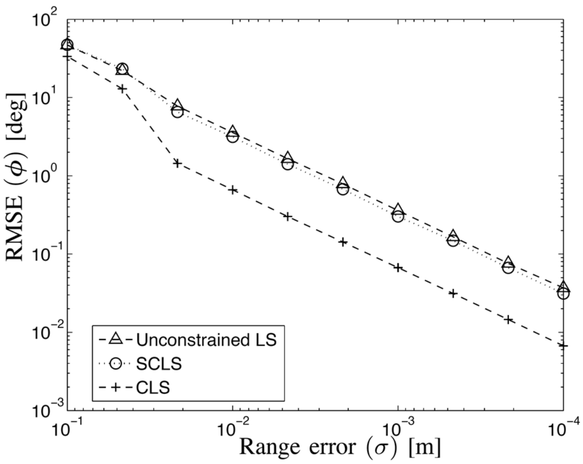

(b)

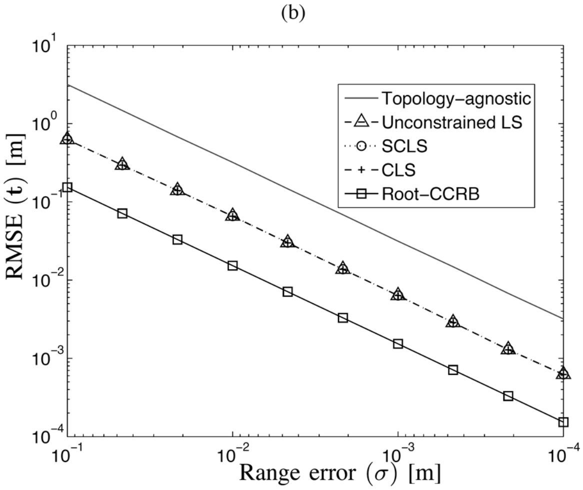

(c)

Fig. 3. Effect of bad anchor geometry ($\mathrm{cond}(\mathbf{A}) = 100$): (a) RMSE of the estimated rotation matrix $\mathbf{Q}$. (b) RMSE in degrees of the estimated rotations. (c) RMSE of the estimated translation vector $\mathbf{t}$.

$v_{mn}, m = 1, 2, \ldots, M; n = 1, 2, \ldots, N$, in the vector

$$\mathbf{v} = [v_{11}, v_{12}, \ldots, v_{M1}, \ldots, v_{MN}]^T \in \mathbb{R}^{MN},$$

and $\sigma_{mn}^2, m = 1, 2, \ldots, M; n = 1, 2, \ldots, N$, in the vector

$$\boldsymbol{\mu} = [\sigma_{11}^2, \sigma_{12}^2, \ldots, \sigma_{M1}^2, \ldots, \sigma_{MN}^2]^T \in \mathbb{R}^{MN},$$

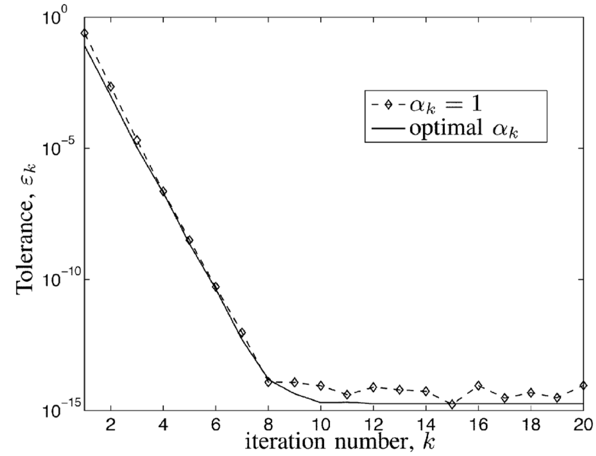

Fig. 4. Convergence of Gauss-Newton iterations for range error $\sigma = 10^{-2}\mathrm{m}$.

we can write (43) compactly as

$$\mathbf{n} = \mathrm{diag}(2\boldsymbol{\rho})\mathbf{v} + \mathbf{v}^{\odot 2} - \boldsymbol{\mu},$$

where

$$\mathbf{n} = [n_{11}, n_{12}, \ldots, n_{M1}, \ldots, n_{MN}]^T \in \mathbb{R}^{MN}.$$

We can then compute the mean of $\mathbf{n}$ as $\mathbb{E}\{\mathbf{n}\} = \mathbf{0}_{MN}$, and the covariance matrix of $\mathbf{n}$ as

$$\begin{aligned}\mathbf{R_n} &= \mathbb{E}\{(\mathbf{n} - \mathbb{E}\{\mathbf{n}\})(\mathbf{n} - \mathbb{E}\{\mathbf{n}\})^T\} \\ &= \mathrm{diag}(2\boldsymbol{\rho})\mathbf{R_v}\mathrm{diag}(2\boldsymbol{\rho}) + \mathbf{R}_{\mathbf{v}^{\odot 2}} - \boldsymbol{\mu}\boldsymbol{\mu}^T \in \mathbb{R}^{MN \times MN},\end{aligned}$$

where

$$\mathbf{R_v} = \mathrm{diag}(\boldsymbol{\mu}) \in \mathbb{R}^{MN \times MN},$$

and

$$\mathbf{R}_{\mathbf{v}^{\odot 2}} = \begin{bmatrix} 3\sigma_{11}^4 & \sigma_{11}^2\sigma_{12}^2 & \cdots & \sigma_{11}^2\sigma_{MN}^2 \\ \sigma_{11}^2\sigma_{12}^2 & 3\sigma_{12}^4 & \cdots & \vdots \\ \vdots & \cdots & \ddots & \vdots \\ \sigma_{11}^2\sigma_{MN}^2 & \cdots & \cdots & 3\sigma_{MN}^4 \end{bmatrix} \in \mathbb{R}^{MN \times MN}.$$

APPENDIX B
GAUSS-NEWTON ITERATIONS ON THE STIEFEL MANIFOLD

The Newton method to solve the WOPP is developed in [23], and it is adapted to suit our problem. In this section, we derive the Gauss-Newton iterations to solve the LS problems on the Stiefel manifold.

The CLS and CTLS problems solve an optimization problem on the Stiefel manifold of the form

$$\arg\min_{\mathbf{Q}} \quad \|\mathbf{z} - \mathbf{L}\mathrm{vec}(\mathbf{Q})\|_2^2 \quad \text{s.t.} \quad \mathbf{Q} \in \mathcal{V}_{3,3}. \tag{44}$$

We can represent any unitary matrix $\mathbf{Q}$ in the vicinity of a given unitary matrix $\mathbf{Q}_k$ as

$$\mathbf{Q} = \mathbf{Q}_k\boldsymbol{\Omega}(\mathbf{x}), \tag{45}$$

where the operator $\boldsymbol{\Omega}(\cdot) : \mathbb{R}^3 \to \mathcal{V}_{3,3}$ is defined as

$$\boldsymbol{\Omega}(\mathbf{x}) = \exp(\mathbf{X}(\mathbf{x})), \tag{46}$$

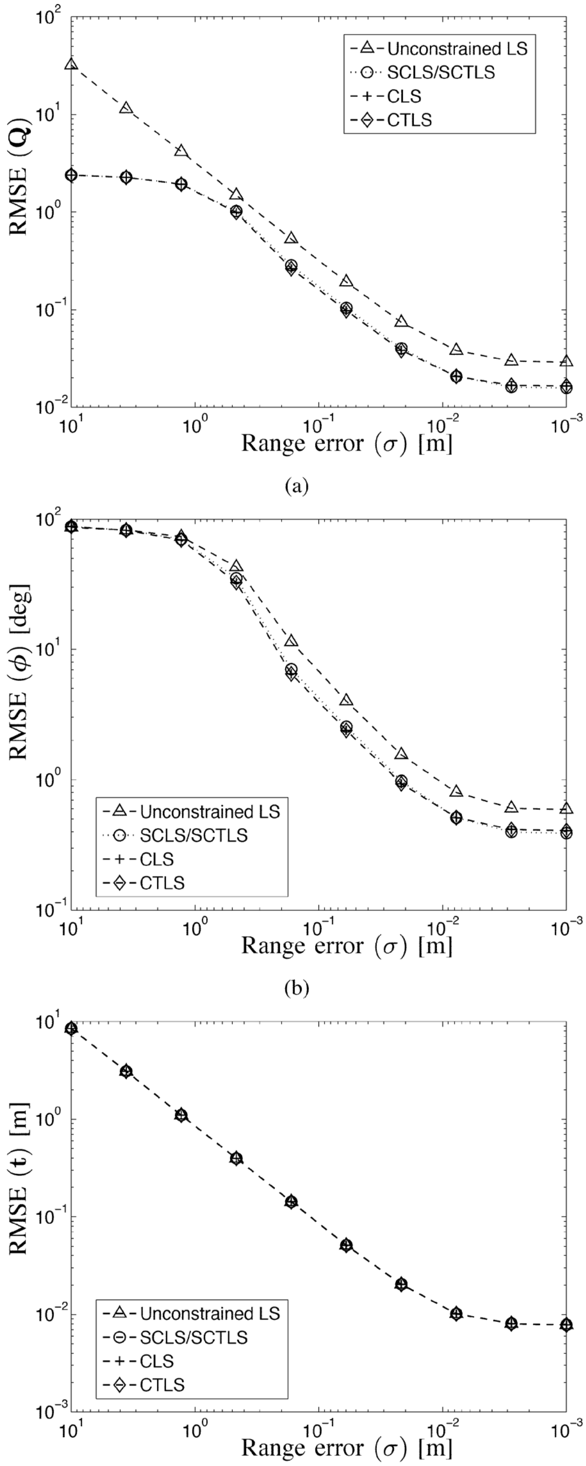

Fig. 5. Results for a perturbed topology $\mathbf{C}$. We use $\sigma_e = 1$ cm. (a) RMSE of the estimated rotation matrix $\mathbf{Q}$. (b) RMSE in degrees of the estimated rotations. (c) RMSE of the estimated translation vector $\mathbf{t}$.

and $\mathbf{X}(\mathbf{x})$ is a skew-symmetric matrix

$$\mathbf{X}(\mathbf{x}) = \begin{bmatrix} 0 & -x_1 & -x_2 \\ x_1 & 0 & -x_3 \\ x_2 & x_3 & 0 \end{bmatrix} \in \mathbb{R}^{3\times 3},$$

with $\mathbf{x} = [x_1, x_2, x_3]^T \in \mathbb{R}^{3\times 1}$. We use the matrix exponential $\exp(\mathbf{X})$ to map a point $\mathbf{x} \in \mathbb{R}^3$ onto the Stiefel manifold $\mathcal{V}_{3,3}$.

We linearize the matrix exponential by using a first-order expansion of the matrix exponential

$$\mathbf{\Omega}(\mathbf{x}) \approx \mathbf{I}_3 + \mathbf{X}.$$

Using this linearization[3] in (45) we get

$$\mathbf{Q} \approx \mathbf{Q}_k(\mathbf{I}_3 + \mathbf{X}).$$

We can then express $\mathbf{L}\mathrm{vec}(\mathbf{Q})$ as

$$\mathbf{L}\mathrm{vec}(\mathbf{Q}) \approx \mathbf{L}\mathrm{vec}(\mathbf{Q}_k) + \mathbf{L}\mathrm{vec}(\mathbf{Q}_k\mathbf{X}),$$

which is a function of $\mathbf{x}$, i.e.,

$$f_k(\mathbf{x}) = \mathbf{L}\mathrm{vec}(\mathbf{Q}_k) + \mathbf{J}\mathbf{x}, \tag{47}$$

where

$$\mathbf{J} = \frac{\partial \mathbf{L}\mathrm{vec}(\mathbf{Q}_k\mathbf{X})}{\partial \mathbf{x}^T} \in \mathbb{R}^{K\times 3}. \tag{48}$$

Next, we solve the optimization problem in (44) iteratively as follows. Using (47) in (44), we can transform the unitarily constrained optimization problem into an unconstrained minimization problem. More specifically, during the k-th iteration we compute the Gauss-Newton search direction by minimizing the following unconstrained LS problem

$$\begin{aligned} \mathbf{x}_k &= \arg\min_{\mathbf{x}\in\mathbb{R}^3} \quad \psi(\mathbf{x}) = \|\mathbf{z} - f_k(\mathbf{x})\|_2^2 \\ &= (\mathbf{J}^T\mathbf{J})^{-1}\mathbf{J}^T(\mathbf{z} - \mathbf{L}\mathrm{vec}(\mathbf{Q}_k)), \end{aligned} \tag{49}$$

and subsequently compute the rotation update

$$\mathbf{Q}_{k+1} = \mathbf{Q}_k\mathbf{\Omega}(\alpha_k\mathbf{x}_k).$$

Here, α_k is the step size. The optimal step size is obtained by solving

$$\alpha_k = \arg\min_{\alpha\in(0,1]} \quad \|\mathbf{z} - \mathbf{L}\mathrm{vec}(\mathbf{Q}_k\mathbf{\Omega}(\alpha\mathbf{x}_k))\|_2^2, \tag{50}$$

whose solution is the root of the polynomial equation obtained by expanding the matrix exponential [23], or can be computed simply by line search. With a good initial point and at low noise levels we can take $\alpha_k = 1$.

The solution $\widehat{\mathbf{Q}}_{\mathrm{SCLS}}$ of the SCLS algorithm can be used as an initial point for the iterative algorithm. Alternatively, the initial point can be computed by orthonormalizing the solution of the unconstrained LS solution $\widehat{\mathbf{Q}}_{\mathrm{LS}}$. The latter orthonormalization procedure solves a special case of OPP, and is given as

$$\begin{aligned} \mathbf{Q}_0 &:= \arg\min_{\mathbf{Q}} \|\mathbf{Q} - \widehat{\mathbf{Q}}_{\mathrm{LS}}\|_F^2 \quad \text{s.t.} \quad \mathbf{Q}^T\mathbf{Q} = \mathbf{I}_3 \\ &= (\widehat{\mathbf{Q}}_{\mathrm{LS}}\widehat{\mathbf{Q}}_{\mathrm{LS}}^T)^{-1/2}\widehat{\mathbf{Q}}_{\mathrm{LS}}. \end{aligned} \tag{51}$$

[3]Instead of a matrix exponential, a Cayley transformation $\mathbf{\Omega}(\mathbf{x}) = (\mathbf{I}_3 + \mathbf{X})(\mathbf{I}_3 + \mathbf{X})^{-1}$ can be alternatively used, which can be then linearized by using a first-order expansion of $(\mathbf{I}_3 + \mathbf{X})^{-1} \approx \mathbf{I}_3 + \mathbf{X}$ (see [23]). As a result, we get a similar expression $\mathbf{Q} \approx \mathbf{Q}_k(\mathbf{I}_3 + 2\mathbf{X})$.

$$\begin{bmatrix}\bar{\mathbf{e}}\\ \tilde{\mathbf{n}}\end{bmatrix} = -\begin{bmatrix}(\mathbf{I}_{3(N-1)} \otimes \mathbf{Q}^T\bar{\mathbf{A}}^T)\\ -\mathbf{I}_K\end{bmatrix}((\mathbf{I}_{3(N-1)} \otimes \bar{\mathbf{A}}\bar{\mathbf{A}}^T) + \mathbf{I}_K)^{-1}[(\mathbf{I}_{3(N-1)} \otimes \bar{\mathbf{A}}\mathbf{Q}) \mid -\mathbf{I}_K]\begin{bmatrix}\bar{\mathbf{c}}\\ \tilde{\mathbf{d}}\end{bmatrix}. \tag{56}$$

APPENDIX C
PROOF OF THEOREM 2

We prove the claim of Theorem 2 by contradiction. Let there exist an unbiased constrained estimator $\widehat{\mathbf{Q}}$ such that $\widehat{\mathbf{Q}} \in \mathcal{V}_{3,3}$. Then $\widehat{\mathbf{Q}} = \mathbf{Q} + \mathbf{\Psi}$ where $\mathbf{\Psi}$ is the estimation error such that $\mathbb{E}\{\widehat{\mathbf{Q}}\} = \mathbf{Q}$ or $\mathbb{E}\{\mathbf{\Psi}\} = \mathbf{0}$. Since $\widehat{\mathbf{Q}} \in \mathcal{V}_{3,3}$, we have $\widehat{\mathbf{Q}}\widehat{\mathbf{Q}}^T = \mathbf{I}_3$, and hence

$$(\mathbf{Q} + \mathbf{\Psi})(\mathbf{Q} + \mathbf{\Psi})^T = \mathbf{I}_3. \tag{52}$$

Using $\mathbf{Q}\mathbf{Q}^T = \mathbf{I}_3$ and taking expectations on both sides, (52) can be further simplified to

$$\mathrm{tr}\{\mathbb{E}\{\mathbf{\Psi}\}\mathbf{Q}^T\} + \mathrm{tr}\{\mathbf{Q}\mathbb{E}\{\mathbf{\Psi}^T\}\} = -\mathbb{E}\{\|\mathbf{\Psi}\|_F^2\}. \tag{53}$$

Due to the assumption that $\mathbb{E}\{\mathbf{\Psi}\} = \mathbf{0}$, the left-hand side of (53) is zero, but, the right-hand side is strictly less than zero. Hence a contradiction occurs, unless the noise is zero. □

APPENDIX D
PROOF OF THEOREM 3

The proof from [18] is provided here to aid the understanding of the proof of the next theorem. For any $\mathbf{Q}$, we can re-write the constraint in (36) as

$$[\mathbf{Q} \mid -\mathbf{I}_3]\begin{bmatrix}\bar{\mathbf{E}}\\ \check{\mathbf{N}}\end{bmatrix} = -[\mathbf{Q} \mid -\mathbf{I}_3]\begin{bmatrix}\bar{\mathbf{C}}\\ \check{\mathbf{D}}\end{bmatrix}.$$

Using the unitary constraint on $\mathbf{Q}$, and pseudo-inverting the wide matrix $[\mathbf{Q} \mid -\mathbf{I}_{3(N-1)}]$ we get

$$\begin{aligned}\begin{bmatrix}\bar{\mathbf{E}}\\ \check{\mathbf{N}}\end{bmatrix} &= -\frac{1}{2}\begin{bmatrix}\mathbf{Q}^T\\ -\mathbf{I}_3\end{bmatrix}[\mathbf{Q} \mid -\mathbf{I}_3]\begin{bmatrix}\bar{\mathbf{C}}\\ \check{\mathbf{D}}\end{bmatrix}\\ &= -\frac{1}{2}\begin{bmatrix}\mathbf{I}_3 & -\mathbf{Q}^T\\ -\mathbf{Q} & \mathbf{I}_3\end{bmatrix}\begin{bmatrix}\bar{\mathbf{C}}\\ \check{\mathbf{D}}\end{bmatrix}\\ &= -\frac{1}{2}\begin{bmatrix}\bar{\mathbf{C}} - \mathbf{Q}^T\check{\mathbf{D}}\\ \check{\mathbf{D}} - \mathbf{Q}\bar{\mathbf{C}}\end{bmatrix}.\end{aligned}$$

We can now re-write the objective in (36) to compute the minimum-norm square solution

$$\begin{aligned}&\mathrm{tr}\left\{[\bar{\mathbf{E}}^T \mid \check{\mathbf{N}}^T]\begin{bmatrix}\bar{\mathbf{E}}\\ \check{\mathbf{N}}\end{bmatrix}\right\}\\ &= \frac{1}{2}\mathrm{tr}(\bar{\mathbf{C}}^T\bar{\mathbf{C}} - \check{\mathbf{D}}^T\mathbf{Q}\bar{\mathbf{C}} - \bar{\mathbf{C}}^T\mathbf{Q}^T\check{\mathbf{D}} + \check{\mathbf{D}}^T\check{\mathbf{D}})\\ &= \frac{1}{2}\|\bar{\mathbf{C}}\|_F^2 - \mathrm{tr}(\mathbf{Q}\bar{\mathbf{C}}\check{\mathbf{D}}^T) + \frac{1}{2}\|\check{\mathbf{D}}\|_F^2.\end{aligned}$$

The solution to the SCTLS problem is then obtained by optimizing the term depending only on $\mathbf{Q}$, i.e., by maximizing $\mathrm{tr}\{\mathbf{Q}\bar{\mathbf{C}}\check{\mathbf{D}}^T\}$. This is the same cost as that of the SCLS problem (see [22, pg. 601]). Hence, the solution to the unitarily constrained TLS problem is

$$\widehat{\mathbf{Q}}_{\mathrm{SCTLS}} = \mathbf{V}\mathbf{U}^T, \tag{54}$$

where the matrices $\mathbf{V}$ and $\mathbf{U}$ are obtained by computing the SVD of $\check{\mathbf{D}}\bar{\mathbf{C}}^T = \mathbf{V}\mathbf{\Sigma}\mathbf{U}^T$. □

APPENDIX E
PROOF OF THEOREM 4

For any $\mathbf{Q}$ the constraint in the optimization problem (39) can be written as

$$\begin{aligned}&[(\mathbf{I}_{3(N-1)} \otimes \bar{\mathbf{A}}\mathbf{Q}) \mid -\mathbf{I}_K]\begin{bmatrix}\bar{\mathbf{e}}\\ \tilde{\mathbf{n}}\end{bmatrix}\\ &\qquad = -[(\mathbf{I}_{3(N-1)} \otimes \bar{\mathbf{A}}\mathbf{Q}) \mid -\mathbf{I}_K]\begin{bmatrix}\bar{\mathbf{c}}\\ \tilde{\mathbf{d}}\end{bmatrix}.\end{aligned} \tag{55}$$

Multiplying both sides of (55) with the pseudo-inverse of the wide-matrix $[(\mathbf{I}_{3(N-1)} \otimes \bar{\mathbf{A}}\mathbf{Q}) \mid -\mathbf{I}_K]$ given by

$$\begin{aligned}&[(\mathbf{I}_{3(N-1)} \otimes \bar{\mathbf{A}}\mathbf{Q}) \mid -\mathbf{I}_K]^\dagger\\ &\quad = \begin{bmatrix}\mathbf{I}_{3(N-1)} \otimes \mathbf{Q}^T\bar{\mathbf{A}}^T\\ -\mathbf{I}\end{bmatrix}((\mathbf{I}_{3(N-1)} \otimes \bar{\mathbf{A}}\bar{\mathbf{A}}^T) + \mathbf{I}_K)^{-1},\end{aligned}$$

we get the minimum-norm solution $\boldsymbol{\epsilon} = [\bar{\mathbf{e}}^T, \tilde{\mathbf{n}}^T]^T$ to the system of equations in (55) which is given by (56) at the top of the page.

Assuming that the covariance matrix of the perturbation vector is a scaled identity matrix, it is straightforward to verify that the objective in (40) using (56) simplifies to

$$\mathrm{tr}\left\{[\bar{\mathbf{e}}^T \mid \tilde{\mathbf{n}}^T]\,\mathbf{R}_{\boldsymbol{\epsilon}}\begin{bmatrix}\bar{\mathbf{e}}\\ \tilde{\mathbf{n}}\end{bmatrix}\right\} = \|\mathbf{\Lambda}^{1/2}(\tilde{\mathbf{d}} - (\bar{\mathbf{C}}^T \otimes \bar{\mathbf{A}})\mathbf{q})\|_2^2,$$

where

$$\begin{aligned}\mathbf{\Lambda}^{1/2} &= (\sigma_{\mathrm{e}}^{-2}(\mathbf{I}_{3(N-1)} \otimes \bar{\mathbf{A}}\bar{\mathbf{A}}^T) + \mathbf{R}_{\tilde{\mathbf{n}}}^{-1})^{1/2}\\ &\qquad ((\mathbf{I}_{3(N-1)} \otimes \bar{\mathbf{A}}\bar{\mathbf{A}}^T) + \mathbf{I}_K)^{-1}.\end{aligned} \tag{57}$$

Hence, the solution to the optimization problem (40) is equivalent to a specifically weighted CLS. □

REFERENCES

[1] S. P. Chepuri, G. Leus, and A.-J. Van der Veen, “Position and orientation estimation of a rigid body: Rigid body localization,” in *Proc. IEEE Int. Conf. Acoust., Speech, Signal Process. (ICASSP)*, May 2013, pp. 5185–5189.

[2] N. Patwari, J. N. Ash, S. Kyperountas, A. O. Hero III, R. L. Moses, and N. S. Correal, “Locating the nodes: cooperative localization in wireless sensor networks,” *IEEE Signal Process. Mag.*, vol. 22, no. 4, pp. 54–69, Jul. 2005.

[3] S. Gezici, Z. Tian, G. B. Giannakis, H. Kobayashi, A. F. Molisch, H. V. Poor, and Z. Sahinoglu, “Localization via ultra-wideband radios: a look at positioning aspects for future sensor networks,” *IEEE Signal Process. Mag.*, vol. 22, no. 4, pp. 70–84, Jul. 2005.

[4] F. Gustafsson and F. Gunnarsson, “Mobile positioning using wireless networks: possibilities and fundamental limitations based on available wireless network measurements,” *IEEE Signal Process. Mag.*, vol. 22, no. 4, pp. 41–53, Jul. 2005.

[5] S. P. Chepuri, R. Rajan, G. Leus, and A.-J. Van der Veen, “Joint clock synchronization and ranging: Asymmetrical time-stamping and passive listening,” *IEEE Signal Process. Lett.*, vol. 20, no. 1, pp. 51–54, Jan. 2013.

[6] S. P. Chepuri, G. Leus, and A.-J. Van der Veen, “Joint localization and clock synchronization for wireless sensor networks,” in *Conf. Rec. 46th Asilomar Conf. Signals, Syst., Comput. (ASILOMAR)*, Nov. 2012, pp. 1432–1436.

[7] K. W. Cheung and H. C. So, “A multidimensional scaling framework for mobile location using time-of-arrival measurements,” *IEEE Trans. Signal Process*, vol. 53, no. 2, pp. 460–470, Feb. 2005.

[8] J. A. Costa, N. Patwari, and A. O. Hero III, “Distributed weighted-multidimensional scaling for node localization in sensor networks,” *ACM Trans. Sensors Netw.*, vol. 2, no. 1, pp. 39–64, Feb. 2006.

[9] L. Salhuana, “Tilt sensing using linear accelerometers,” Freescale Semiconductor—Application Note, Appl. Note AN3461, Feb. 2012.

[10] J. D. Hol, F. Dijkstra, H. Luinge, and T. B. Schon, “Tightly coupled UWB/IMU pose estimation pose estimation,” in *Proc. IEEE Int. Conf. Ultra-Wideband (ICUWB)*, 2009, pp. 688–692.

[11] J. D. Hol, “Sensor fusion and calibration of inertial sensors, vision, ultra-wideband and GPS,” *Dissertations Linköping Stud. Sci. Technol.*, vol. 1368, 2011.

[12] G. Wahba, “A least squares estimate of satellite attitude,” *SIAM Rev.*, vol. 7, no. 3, pp. 409–409, 1965.

[13] C. Cohen, “Attitude determination using GPS,” Ph.D. dissertation, Aeronautics and Astronautics Dept., Stanford Univ., Stanford, CA, USA, 1992.

[14] J.-C. Juang and G.-S. Huang, “Development of GPS-based attitude determination algorithms,” *IEEE Trans. Aerosp. Electron. Syst.*, vol. 33, no. 3, pp. 968–976, Jul. 1997.

[15] S. P. Chepuri, A. Simonetto, G. Leus, and A.-J. Van der Veen, “Tracking position and orientation of a mobile rigid body,” in *Proc. IEEE Workshop Comput. Adv. Multi-Sensor Adapt. Process. (CAMSAP)*, Dec. 2013, pp. 37–40.

[16] L. Eldén and H. Park, “A Procrustes problem on the Stiefel manifold,” *Numer. Math.*, vol. 82, pp. 599–619, 1999, 10.1007/s002110050432.

[17] N. A. Chaturvedi, A. K. Sanyal, and N. H. Mc Clamroch, “Rigid-body attitude control,” *IEEE Control Syst. Mag.*, vol. 31, no. 3, pp. 30–51, Jun. 2011.

[18] K. Arun, “A unitarily constrained total least squares problem in signal processing,” *SIAM J. Matrix Anal. Appl.*, vol. 13, no. 3, pp. 729–745, 1992.

[19] B. K. P. Horn, H. M. Hilden, and S. Negahdaripour, “Closed-form solution of absolute orientation using orthonormal matrices,” *J. Opt. Soc. Amer. A*, vol. 5, no. 7, pp. 1127–1135, 1988.

[20] B. K. P. Horn, “Closed-form solution of absolute orientation using unit quaternions,” *J. Opt. Soc. Amer. A*, vol. 4, no. 4, pp. 629–642, 1987.

[21] S. P. Chepuri, G. Leus, and A.-J. Van der Veen, “Sparsity-exploiting anchor placement for localization in sensor networks,” in *Proc. 21st Eur. Signal Process. Conf. (EUSIPCO)*, Sep. 2013, pp. 1–5.

[22] G. H. Golub and C. F. V. Loan*, Matrix Computations, Johns Hopkins Studies in the Mathematical Sciences*. Baltimore, MD, USA: The Johns Hopkins Univ. Press, 1996.

[23] T. Viklands, “Algorithms for the weighted orthogonal procrustes problem and other least squares problems,” Ph.D. dissertation, Comput. Sci. Dept., Umea Univ., Umea, Sweden, 2008.

[24] J. H. Manton, “Optimization algorithms exploiting unitary constraints,” *IEEE Trans. Signal Process.*, vol. 50, no. 3, pp. 635–650, Mar. 2002.

[25] S. M. Kay*, Fundamentals of Statistical Signal Processing: Estimation Theory*. Englewood Cliffs, NJ, USA: Prentice-Hall, 1993.

[26] P. Stoica and B. C. Ng, “On the Cramer-Rao bound under parametric constraints,” *IEEE Signal Process. Lett.*, vol. 5, no. 7, pp. 177–179, Jul. 1998.

[27] J. Diebel, “Representing attitude: Euler angles, unit quaternions, and rotation vectors,” *Matrix*, vol. 58, pp. 15–16, 2006.

Sundeep Prabhakar Chepuri (S’11) was born in India in 1986. He received his B.E. degree (distinction) in electrical engineering from the PES Institute of Technology, Bangalore, India, in 2007, and his M.Sc. degree (*cum laude*) in electrical engineering from the Delft University of Technology, The Netherlands, in 2011. He has held positions at Robert Bosch, India, during 2007–2009, and Holst Centre/imec-nl, The Netherlands, during 2010–2011. Since September 2011, he has been with the Circuits and Systems group at the Faculty of Electrical Engineering, Mathematics and Computer Science of the Delft University of Technology, The Netherlands, pursuing his Ph.D. degree. His research interest lies in the field of signal processing for communications and networks.

Geert Leus (M’01–SM’05–F’12) received the Electrical Engineering degree and the Ph.D. degree in applied sciences from the Katholieke Universiteit Leuven, Belgium, in 1996 and 2000, respectively. Currently, he is an “Antoni van Leeuwenhoek” Full Professor at the Faculty of Electrical Engineering, Mathematics and Computer Science of the Delft University of Technology, Delft, The Netherlands. His research interests are in the area of signal processing for communications.

Prof. Leus received a 2002 IEEE Signal Processing Society Young Author Best Paper Award and a 2005 IEEE Signal Processing Society Best Paper Award. He was the Chair of the IEEE Signal Processing for Communications and Networking Technical Committee, and an Associate Editor for the IEEE TRANSACTIONS ON SIGNAL PROCESSING, the IEEE TRANSACTIONS ON WIRELESS COMMUNICATIONS, and the IEEE SIGNAL PROCESSING LETTERS. Currently, he is a member of the IEEE Sensor Array and Multichannel Technical Committee and serves as the Editor in Chief of the *EURASIP Journal on Advances in Signal Processing*.

Alle-Jan van der Veen (M’95–SM’03–F’05) was born in The Netherlands in 1966. He received the Ph.D. degree (*cum laude*) from TU Delft, The Netherlands, in 1993. At present, he is a Full Professor and head of the Circuits and Signals group at the Department of Electrical Engineering, Mathematics and Computer Science, TU Delft, The Netherlands. His research interests are in the general area of system theory applied to signal processing, and in particular algebraic methods for array signal processing, with applications to wireless communications and radio astronomy.

Prof. Van der Veen is the recipient of a 1994 and a 1997 IEEE Signal Processing Society (SPS) Young Author paper award. He was an Associate Editor for IEEE TRANSACTIONS ON SIGNAL PROCESSING (1998–2001), chairman of the IEEE SPS Signal Processing for Communications Technical Committee (2002–2004), Editor-in-Chief of IEEE SIGNAL PROCESSING LETTERS (2002–2005) and Editor-in-Chief of IEEE TRANSACTIONS ON SIGNAL PROCESSING (2006–2008). He was an elected member-at-large of the Board of Governors of IEEE SPS (2006–2008), member of the IEEE SPS Awards Board, chairman of the IEEE SPS Fellow Reference Committee, and member of the IEEE TAB Periodicals Review and Advice Committee.